AFAPL-TR-75-71

CAN-TYPE COMBUSTOR DESIGN FOR A LOW COST SUBSONIC RAMJET ENGINE

DECEMBER 1975

TECHNICAL REPORT AFAPL-TR-75-71
FINAL REPORT FOR PERIOD 1 APRIL 1974 – 1 APRIL 1975

Approved for public release; distribution unlimited

AIR FORCE AERO PROPULSION LABORATORY
AIR FORCE WRIGHT AERONAUTICAL LABORATORIES
Air Force Systems Command
Wright-Patterson Air Force Base, Ohio 45433

NOTICE

When Government drawings, specifications, or other data are used for any purpose other than in connection with a definitely related Government procurement operation, the United States Government thereby incurs no responsibility nor any obligation whatsoever; and the fact that the Government may have formulated, furnished, or in any way supplied the said drawings, specifications, or other data, is not to be regarded by implication or otherwise as in any manner licensing the holder or any other person or corporation, or conveying any rights or permission to manufacture, use, or sell any patented invention that may in any way be related thereto.

This report contains the results of an effort to design, fabricate, and test a can-type combustor for the low cost subsonic ramjet. The work was performed in the Ramjet Engine Division of the Air Force Aero Propulsion Laboratory, Air Force Systems Command, Wright-Patterson AFB, Ohio under Project 3012, Task 301208, and Work Unit 30120829. The effort was conducted by 1Lt Charles E. Hornbeck during the period April 1974 to April 1975.

This report has been reviewed by the Information Office, (ASD/OIP) and is releasable to the National Technical Information Service (NTIS). At NTIS, it will be available to the general public, including foreign nations.

This Technical report has been reviewed and is approved for publication.

Charles E Hornbeck

CHARLES E. HORNBECK, 1Lt, USAF
Project Engineer

FOR THE COMMANDER

William E Supp

WILLIAM E. SUPP, Technical Manager
Strategic Missile Propulsion

Copies of this report should not be returned unless return is required by security considerations, contractual obligations, or notice on a specific document.

UNCLASSIFIED

SECURITY CLASSIFICATION OF THIS PAGE (When Data Entered)

REPORT DOCUMENTATION PAGE

READ INSTRUCTIONS BEFORE COMPLETING FORM

1. REPORT NUMBER: AFAPL-TR-75-71

2. GOVT ACCESSION NO.

3. RECIPIENT'S CATALOG NUMBER

4. TITLE (and Subtitle): CAN-TYPE COMBUSTOR DESIGN FOR A LOW COST SUBSONIC RAMJET ENGINE.

5. TYPE OF REPORT & PERIOD COVERED: Technical Report (Final) 1 Apr 1974 - 1 Apr 1975

6. PERFORMING ORG. REPORT NUMBER

7. AUTHOR(s): Charles E. Hornbeck, 1Lt, USAF

8. CONTRACT OR GRANT NUMBER(s)

9. PERFORMING ORGANIZATION NAME AND ADDRESS: Air Force Aero Propulsion Laboratory (RJA), Wright-Patterson AFB, OH 45433

10. PROGRAM ELEMENT, PROJECT, TASK AREA & WORK UNIT NUMBERS: Project 3012, Task 301208, Work Unit 30120829

11. CONTROLLING OFFICE NAME AND ADDRESS: Air Force Aero Propulsion Laboratory (RJA), Wright-Patterson AFB, OH 45433

12. REPORT DATE: December 1975

13. NUMBER OF PAGES: 83

14. MONITORING AGENCY NAME & ADDRESS (if different from Controlling Office)

15. SECURITY CLASS. (of this report): Unclassified

15a. DECLASSIFICATION/DOWNGRADING SCHEDULE

16. DISTRIBUTION STATEMENT (of this Report)

Approved for public release; distribution unlimited.

17. DISTRIBUTION STATEMENT (of the abstract entered in Block 20, if different from Report)

18. SUPPLEMENTARY NOTES

19. KEY WORDS (Continue on reverse side if necessary and identify by block number)

Subsonic Ramjets
Can-Type Combustor
Ramjet Combustion Performance

20. ABSTRACT (Continue on reverse side if necessary and identify by block number)

This study investigates the feasibility of using a low cost can combustor in a subsonic ramjet engine in the flight envelope of Mach 0.7 to 0.9, altitude 20,000 to 30,000 feet. A simple can combustor without close fabrication tolerances was designed and fabricated. The can was installed in a subsonic ramjet which was ground tested in a direct-connect pipe set-up.

The combustion efficiency and thrust were determined at conditions representative of the flight envelope. These results are compared with

DD FORM 1 JAN 73 1473 EDITION OF 1 NOV 65 IS OBSOLETE

UNCLASSIFIED

SECURITY CLASSIFICATION OF THIS PAGE (When Data Entered)

results of a model subsonic ramjet engine cycle analysis. The end result of the program is a developed combustor system for a subsonic ramjet which is an inexpensive and attractive propulsion device for one-mission remotely piloted vehicles and target drones.

TABLE OF CONTENTS

LIST OF ILLUSTRATIONS

LIST OF ILLUSTRATIONS (Concluded)

LIST OF TABLES

LIST OF SYMBOLS

A	Cross-Sectional area, ft^2
C_{DB}	Combustor drag coefficient $\equiv D_b/0.5\gamma_2 P_2 A_2 M_2^2$
C_F	Thrust coefficient $\equiv F_{NJ}/0.5\gamma_o P_o A_o M_o^2$
C_{N_D}	Exit nozzle mass flow discharge coefficient
d	Hole diameter, ft
f/a	Ratio of mass rate of fuel flow to mass rate of air flow
F_{NJ}	Net jet thrust, lb_f
g	Gravitational constant, 32.174 $ft\text{-}lb_m/lb_f\text{-}sec^2$
K_T	Inlet air temperature correction factor
L	Length, ft
$\mathring{m}$	Mass flow function $\equiv g\sqrt{\frac{\gamma}{Rg}}\ M\ \left[1 + \frac{\gamma - 1}{2} M^2\right]^{1/2}$
M	Mach number
MW	Molecular weight
P	Static pressure, psia
P_T	Stagnation (or total) pressure, psia
R	Gas constant, $ft\text{-}lb_f/lb_m\text{-}°R$
SFC	Specific fuel consumption, $lb_m/hr\text{-}lb_f$
T	Static temperature, °R
T_T	Stagnation (or total) temperature, °R
$\Delta_{T_{T_I}}$	Ideal temperature rise, °R
Vol	Volume, ft^3
V	Average velocity, ft/sec
$\dot{W}$	Mass flow, lb_m/sec
$\dot{W}_A$	Air flow, lb_m/sec

LIST OF SYMBOLS (Concluded)

$\dot{W}_F$	Fuel flow, lb_m/sec
X	Mach function $\equiv M\sqrt{\gamma} \Big/ \left[1 + \frac{\gamma - 1}{2} M^2\right]^{\frac{\gamma + 1}{2(\gamma - 1)}}$
Y	Mach function $\equiv X/Z$
Z	Mach function $\equiv \left[1 + \gamma M^2\right] \Big/ \left[1 + \frac{\gamma - 1}{2} M^2\right]^{\frac{\gamma}{\gamma - 1}}$
ρ	Density, lb_m/ft^3
γ	Ratio of specific heats
n_c	Thermal combustion efficiency

Subscripts

0-5	Engine stations (see Figure 1)
ALT	Altitude condition
I	Ideal condition
D	Disk plane
j	Jet through combustor holes
S	Stage of holes
T	Stagnation (or total) state
P	Pilot flameholder
M	Main flameholder
rz	Recirculation zone

TABLE OF CONTENTS

processes is the increase of momentum of the air and fuel, resulting in a thrust force.

Because of the simplicity of the ramjet, it can be produced for a very low cost, making it an attractive propulsion device for one-mission designed tactical missiles. Recently there has been a great deal of interest in remotely piloted vehicles and target drones in the subsonic flight speed regime as shown in Figure 2. Because the accomplishment of the air compression is entirely done by fluid dynamic means, the ramjet is best suited for high speeds ($M > 2$). However, due to the necessity of low cost for throw-away missiles, the subsonic ramjet, with only modest performance, is still an attractive propulsion device for these one-mission vehicles.

2. STATEMENT OF THE PROBLEM

The purpose of this investigation was to design, fabricate, and experimentally determine the performance of a can-type combustor for use in a subsonic ramjet engine. The subsonic ramjet uses a simple diverging inlet diffuser and a converging exit nozzle, both of which can be designed to be manufactured easily and cheaply. The combustor flameholder therefore becomes the important factor in the performance and cost of the subsonic engine.

In the past, flameholders in subsonic ramjets have been of the so-called bluff-body or gutter type. They consist of hollow cones and V-shaped gutters, as shown in Figure 3. The simplicity and compactness of the design has provided for very low cost. However, adequate thermal

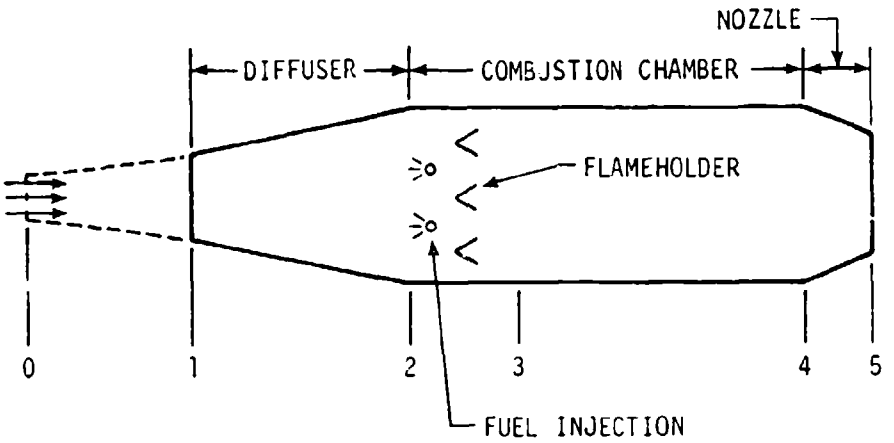

Figure 1. Schematic Diagram of a Subsonic Ramjet Engine

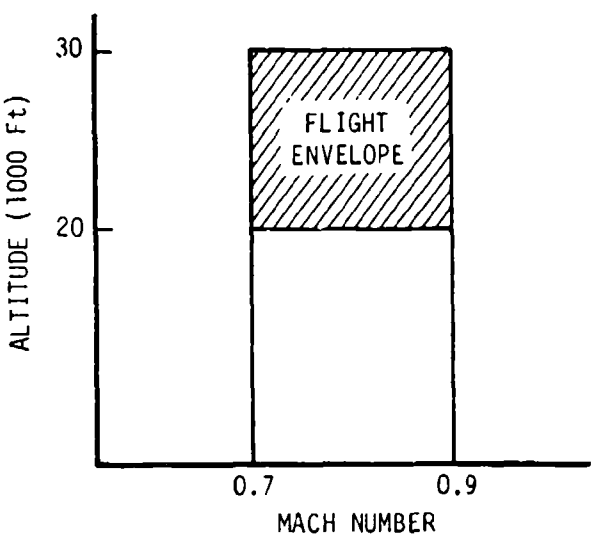

Figure 2. Subsonic Ramjet Flight Envelope

BLUFF-BODY TYPE

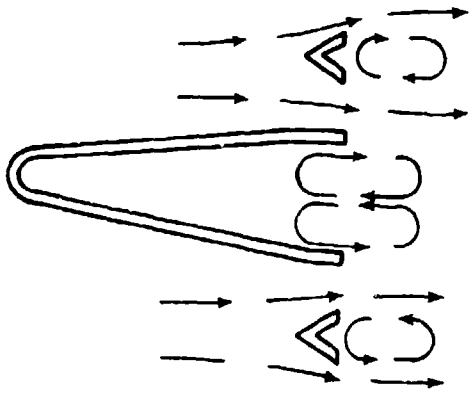

CAN TYPE

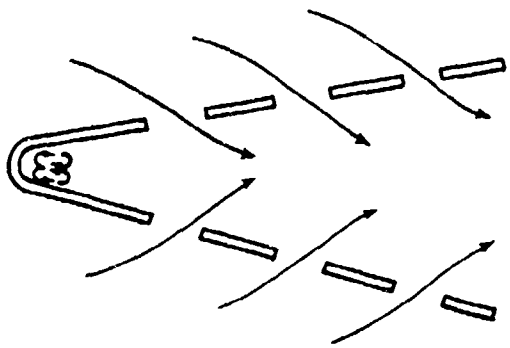

Figure 3. Flameholder Types

combustion efficiencies have not been attainable using bluff-body flameholders.

A can in its simplest form, as shown in Figure 3, is a perforated cone which is actually a multitude of bluff-bodies to hold flame. The separation of the flow of gas through the perforations promotes intense air-fuel mixing and rapid burning. The advantage of the can over the bluff-body flameholder is that the designer has closer control over the distribution of the combustible mixture into the combustion zone. As a result, wider operating limits of fuel-air ratio and higher combustion efficiency are possible over wider ranges of inlet air temperature and pressure. The can flameholder has had its greatest utility as the combustion stabilizer for turbojet engines, where the flameholder cost is not as significant when compared to the total engine cost.

The can's wide operating range makes it a likely solution to the severe operating conditions present in the subsonic ramjet engine. The study described in this report was undertaken to demonstrate that the advantages of the can could be utilized in the subsonic ramjet at a low cost by incorporating a simple design, free of close fabrication tolerance requirements.

3. APPROACH

This study was designed to show whether the concept of low cost can combustors is feasible. The first phase of the study was to design a simple can which would be easy and inexpensive to place in production.

The can was then to be fabricated and tested in a subsonic ramjet engine to determine the combustion performance.

The aspects of combustor performance considered in the design were stability limits, combustion efficiency, and pressure loss. The design of the can is given in detail in Section II. The design is based to an appreciable degree upon completely empirical and semi-theoretical methods. An extensive literature search was conducted to determine the important design considerations. A number of these were incorporated into the can during design. Also, a great deal of redesign was accomplished in the testing portion of the program.

The testing was done in the AF Aero Propulsion Laboratory's Ramjet Test Facility located at Wright-Patterson Air Force Base, Ohio. A description of the test facility, test procedures, measurement instrumentation, and data reduction techniques are given in Section III.

The test results are given in Section IV. The initial testing was to optimize a fuel injection system to maximize the combustion efficiency. Using the optimized fuel injector system, tests were conducted at the Mach number and altitude conditions of the flight envelope of Figure 2. Design changes were incorporated into the can during this phase of testing to provide stable operation at the Mach number and altitude boundaries of the flight envelope. The performance of the can obtained in testing is then compared to the model ramjet performance. Section V presents the final conclusions of the can design study and test program.

SECTION II

CAN-TYPE COMBUSTOR DESIGN

1. GENERAL LAYOUT

The general layout of the can was made by examining the 15-inch diameter low cost ramjet engine of Figure 4. The combustor design chosen contained a two-section conical can flameholder, a pilot can, and a main can (Figures 5 and 6). The pilot can had 6 stages with 8 holes per stage and the main can had 5 stages with 8 holes per stage. As shown, a stage is a row of holes, all in the same plane, which provides an entry path for the fuel-air mixture into the turbulent mixing region of the can. How the number of stages and number of holes per stage was arrived at will be described later in Section II.3. A shroud enclosed the pilot can completely. The shroud divided the air flow for the pilot can from the main can air flow. The pilot can and main can also had separate fuel injection systems upstream to provide a pre-mixed fuel-air mixture. The overall length of the pilot and main can combustor was 47.5 inches with a tailpipe turbulent mixing region of 22.5 inches. This region, with an L/D of 1.5, was needed to allow the combustion process to complete behind the last two stages. A 12-inch length was left between the engine inlet and the shroud inlet plane in order to keep the shroud inlet out of the engine inlet flow field. The diameter of the exit of the main can (Station 3) was 14.0 inches, which allowed a 0.275 gap between the flameholder and the tailpipe. This gap allowed, after thermal expansion of the can flameholder, enough film cooling to prevent a hot spot on the tailpipe. The diameter of the junction of the main and pilot can (Station 2a) was chosen from pressure loss consideration. Grobman (Reference 13) showed for a conical can that the pressure

Figure 4. The Low Cost Subsonic Ramjet

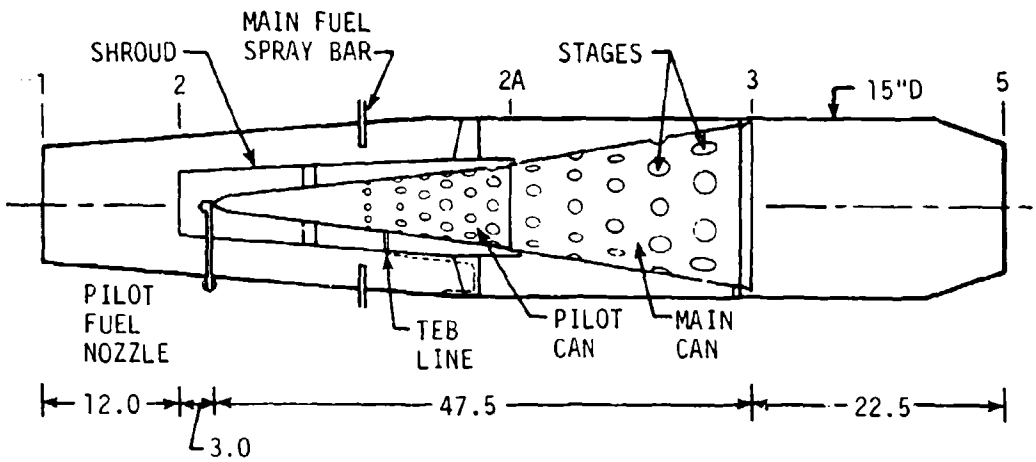

Figure 5. Cross-Section of the Low Cost Subsonic Ramjet with a Can Combustor

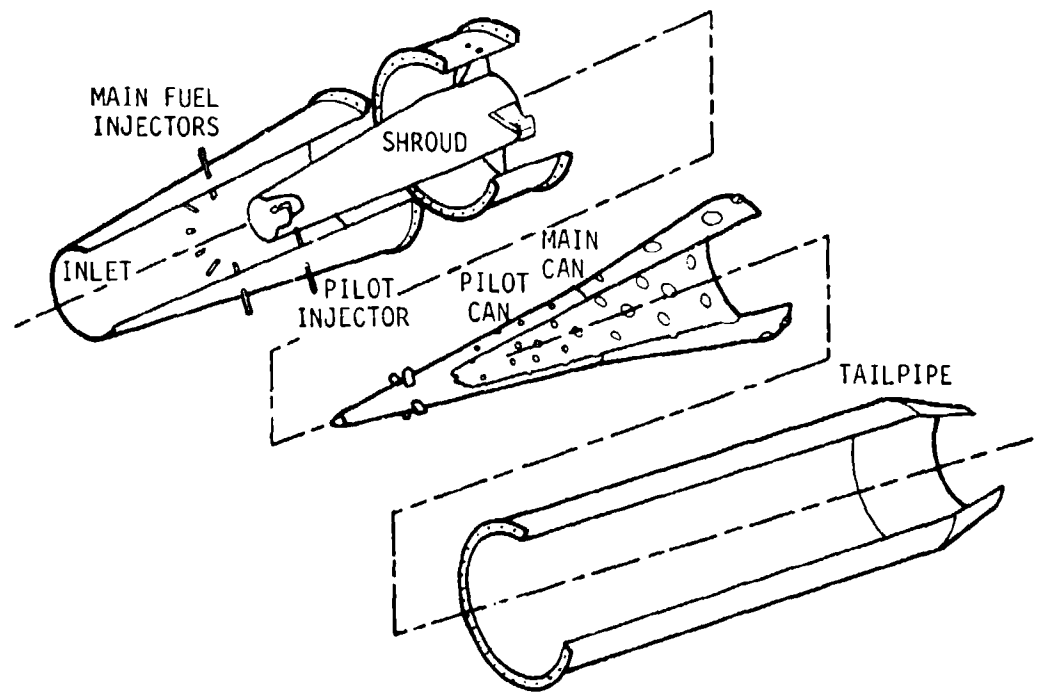

Figure 6. Assembly Drawing of the Low Cost Subsonic Ramjet with a Can Combustor

drop is a minimum when the cross-sectional area just upstream of the first stage of holes is equal to 0.3 of the cross-sectional area of the duct around the flameholder. The diameter at Station 2A, therefore, was 7.0 inches. The same pressure loss consideration was used to obtain a diameter at the pilot can first stage. However, this deals with the subject of pilot stabilization which will be discussed as a separate topic.

2. PILOT STABILIZATION

It was anticipated that it would be difficult to stabilize and maintain a flame in the combustor under the operating conditions of low pressure and temperature. Therefore, it was decided that a flame pilot would be necessary to maintain combustion. This was done by designing the can so that a recirculation zone would appear ahead of the first stage of air entry holes, as shown in Figure 7. This zone was designed to maintain combustion throughout the engine flight envelope. The pilot zone then would maintain the combustion in the remainder of the pilot can which would in turn maintain the combustion in the main can.

The pilot can air flow rate was chosen to be 1/4 of the total engine air flow by designing the shroud inlet (Figure 6) to be 5.5 inches in diameter. This dimension and Grobman's low pressure drop results (Reference 13) of a 0.3 ratio of can cross-sectional area to duct cross-sectional area established the pilot can diameter at the upstream edge of the first stage of holes at 4.0 inches.

To establish the size of the holes of the first stage and the volume of the pilot recirculation zone, the pilot can blow-off data correlation of Figure 8 was used. This is an experimental correlation for 3.0- and 5.0-inch diameter cylindrical pilot can flameholders having one row of holes (Reference 9). In the study described in Reference 9 it was also determined that 16 percent of the first stage fuel-air mixture enters the pilot recirculation zone. The rest of the mixture is burned in the recirculation zone downstream of the holes.

The design of the low cost combustor pilot recirculation zone was performed for the 30,000 feet altitude conditions. These conditions are the most severe due to the lower pressure associated with the higher altitude. The pilot recirculation volume was chosen to be 46.838 cubic inches with 0.5-inch diameter holes in the first stage. The pilot can blow-off data correlation parameter for this design is given in Table I. The effective inlet temperature correction factor, K_T, was used to account for the inlet temperature effect on the flameholding stability. The parameter $\dot{W}_{rz}$ is the fuel-air mixture flow rate entering the pilot recirculation zone volume. The parameter P_{rz} is the pressure of the mixture entering the recirculation zone volume. The value of these parameters becomes known when the fuel-air mixture distribution is decided upon as discussed in the next section. The values given in Table I are for the final design. From Figure 8, it can be determined that this design should provide a stable operating pilot zone in the equivalence ratio operating range of 0.51 to 2.0, which for JP-4 corresponds to the fuel-air ratio in the range of 0.034 to 0.135.

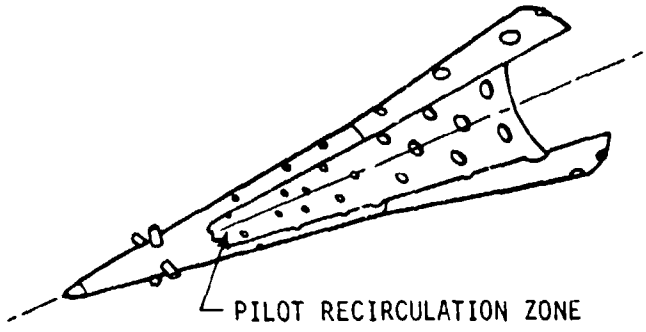

Figure 7. Pilot Recirculation Zone

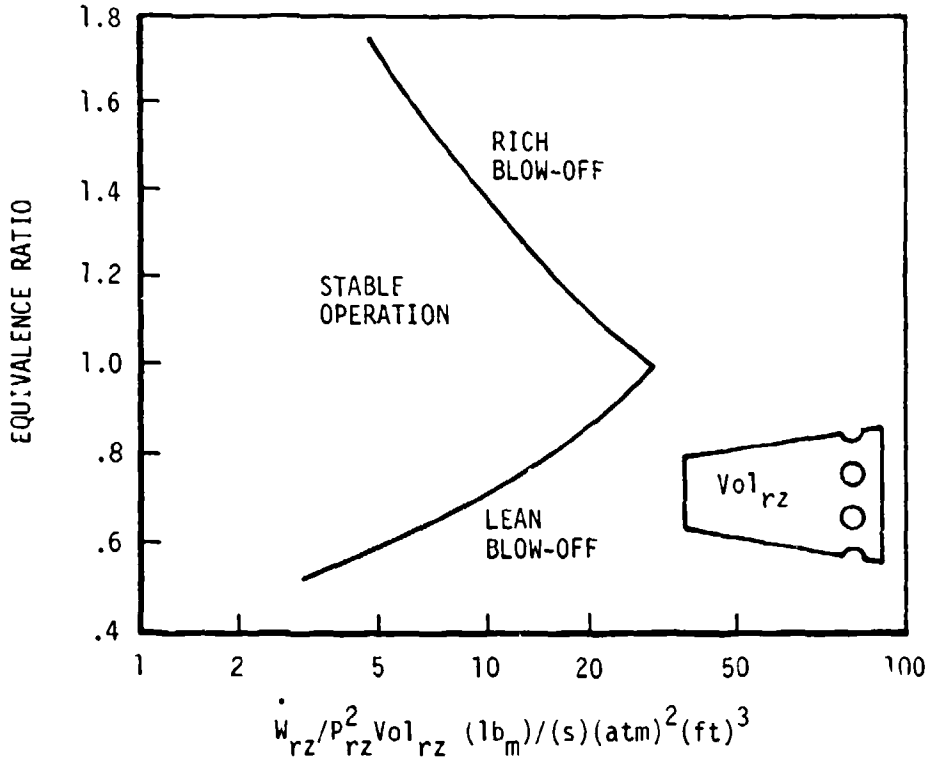

Figure 8. Pilot Can Blow-off Data Correlation
(From Ref. 9)

TABLE I

PILOT BLOW-OFF CORRELATION

Condition	$\frac{\dot{W}_{rz}}{P_{rz}^2 Vol_{rz} K_T}$
M = .7 at 30 KFT	$3.228 \frac{lb_m/sec}{atm^2 ft^3}$
M = .9 at 30 KFT	$2.877 \frac{lb_m/sec}{atm^2 ft^3}$

At the same time the pilot recirculation zone was designed, a design was established also for the remaining stages of the pilot can and the main can. The blow-off data correlation of Zelinski et al (Reference 8) was used and the design is discussed in the next section.

3. FUEL-AIR MIXTURE DISTRIBUTION

The fuel-air mixture should be distributed to the pilot and main can in such a way that each stage of the cans operates at a pressure and velocity which will provide stable operation. The distribution can be controlled by varying the number of hole stages, the number of holes per stage, and the diameter of the holes. There are a number of criteria which have been established from experience which help govern the combinations of the above design variables. These are:

1. Total hole area of entire can should be roughly 120% of combustor cross-sectional area. This leads to a small pressure drop through the holes and to the lowest possible mixture velocity through the holes for a given flow rate (Reference 13).

2. Low pressure drop through the holes and a low velocity are also obtained if each stage has from 40 to 60 percent of its perimeter open (Reference 3).

3. Since too large an addition of reactants after the first stage for a given axial distance may result in quenching of the flame, the minimum distance between stages should be about 2.0 inches (Reference 2).

The above criteria were used to establish a number of possible designs with different hole sizes, different number of stages, and different number of holes per stage. These designs were then evaluated using the blow-off data correlation of Zelinski et al, which is shown in Figure 9.

The design that was finally chosen for the pilot and main can flameholders is shown in Tables II and III. This design was chosen because of its simplicity and because it gave the largest equivalent disk blockage areas (see Figure 9). The large disk blockage would provide large recirculation zones. Low velocities are important so that fuel does not enter the combustion region faster than the combustion reaction can occur. Finally, this design provided the highest mixture pressure through the holes and, therefore, the highest reaction rate.

4. FUEL INJECTION

It is important that the fuel and air mixing process provide a near homogeneous stoichiometric mixture to the can. The combustor design, as shown in Figures 5 and 6, provides for a separate fuel injection system for the pilot and the main cans.

The primary objective of the main fuel injector system is to provide the flameholder element with the proper amount of fuel in a pattern that will result in efficient combustion. The main fuel injectors also provide the capability of varying the overall engine fuel-air ratio in order that the engine thrust level can be varied from acceleration to cruise conditions. With a can flameholder it is important to have a homogeneous fuel-air mixture and not allow the local fuel-air ratio in

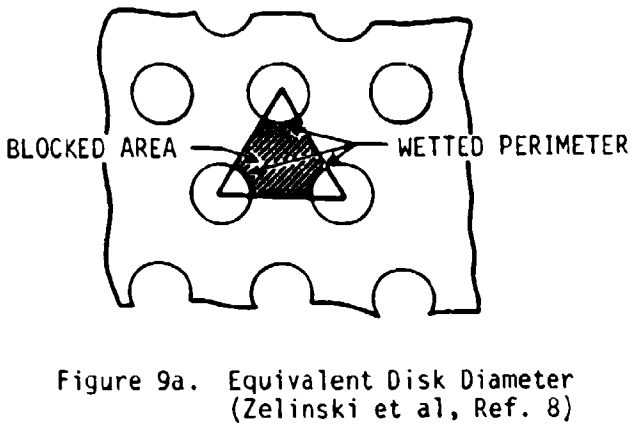

Figure 9a. Equivalent Disk Diameter
(Zelinski et al, Ref. 8)

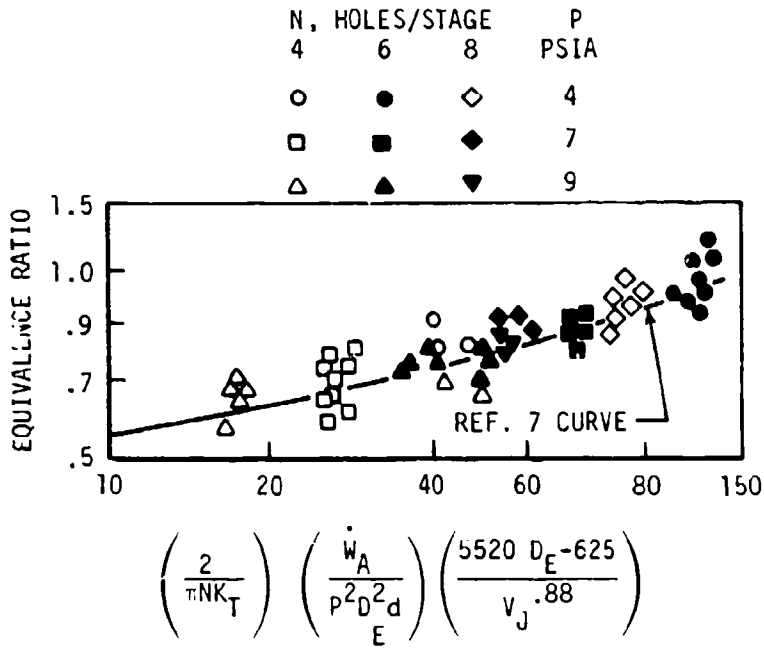

Figure 9b. Blow-off Data Correlation
(Data of Zelinski et al, Ref. 8)

TABLE II

PILOT CAN FLAMEHOLDER DESIGN

Stage	No. of Holes/Stage	Hole Diameter (in.)	Distance to Next Stage (in.)
1	8	0.500	3.0
2	8	0.750	2.0
3	8	1.000	2.0
4	8	1.125	2.0
5	8	1.250	2.0
6	8	1.375	4.0

TABLE III

MAIN CAN FLAMEHOLDER DESIGN

Stage	No. of Holes/Stage	Hole Diameter (in.)	Distance to Next Stage (in.)
1	8	1.500	4.0
2	8	1.750	4.0
3	8	2.000	4.0
4	8	2.250	4.0
5	8	2.500	---

any of the recirculation zones, created behind the can, to become greater than stoichiometric. If the local fuel-air ratio exceeds its stoichiometric value in any zone, then there is more fuel present than can be completely burned and the efficiency is lowered. The main fuel injectors shown in Figure 10 consisted of 12 tubes located circumferentially with each tube having one 0.022-inch diameter spray hole. The 12 injectors were designed so they could be varied in the radial direction. This feature was necessary for the tests described in Section III. For stable combustion, it is important to have a homogeneous fuel-air mixture, in vapor form, without large droplets of fuel. At the conditions at which the engine operates, the inlet temperatures are from -7.8°F to 59.8°F and good fuel vaporization cannot be obtained easily. Therefore, the main fuel injectors were placed such that the fuel spray was directed upstream. This gives the fuel droplets a large relative velocity with respect to the air stream and the droplets break up into smaller droplets. This increases the surface area where evaporation of the fuel can take place.

The pilot fuel injection is not only important for good combustion efficiency, but also for combustion stability of the engine over the entire flight envelope. The pilot fuel injection system also sprays upstream to break up the fuel droplets. To obtain good atomization, two types of spray nozzles were tested (Figure 11). The first type was a full-cone spray nozzle which uses pressure across an orifice to atomize the fuel. The nozzle also contains a swirl plate to give the fuel radial velocity to help facilitate atomization. The second type, a hollow-cone spray nozzle also uses pressure drop across an orifice for

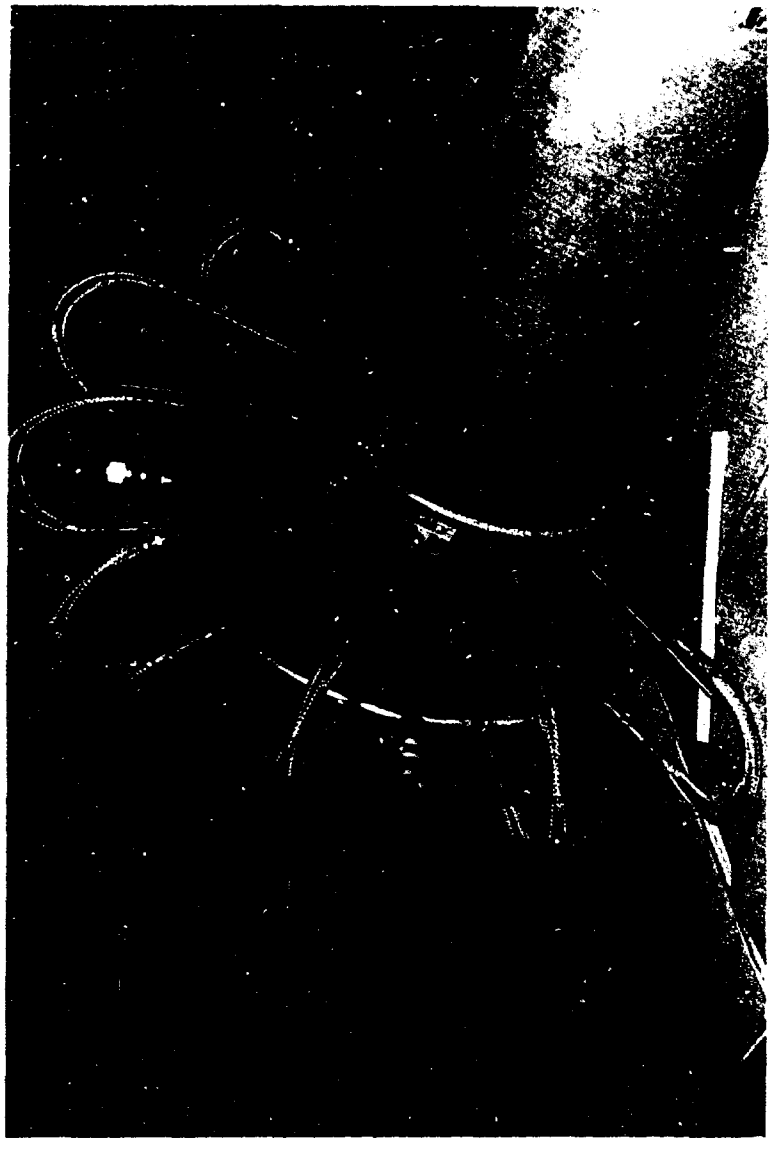

Figure 10. Variable Main Fuel Injectors

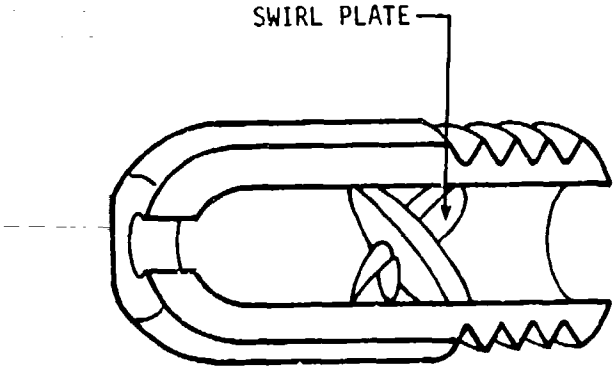

FULL-CONE NOZZLE

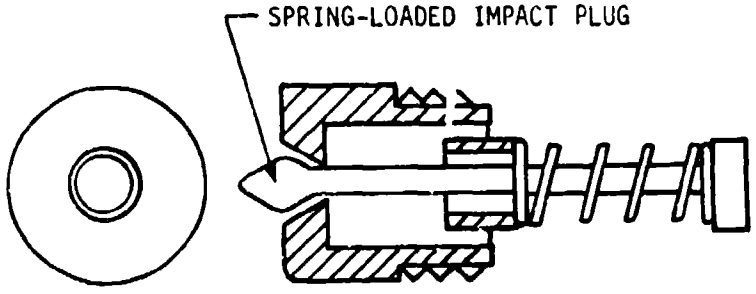

HOLLOW-CONE NOZZLE

Figure 11. Pilot Fuel Injector Types

atomizing. In addition, this nozzle has an impact plug which mechanically facilitates atomization.

Experimental tests were run to define the fuel injection system for optimum combustion efficiency. These tests are described in detail in Section IV.2.

The fuel chosen for this study was JP-4. This fuel was chosen primarily because of its low cost and accessibility. Also, JP-4 has a high heat of combustion, 18,701.3 BTU/lb_m, for good combustion performance and is a volatile fuel even at low temperatures.

5. IGNITION

The engine was ignited by a triethylborane (TEB) ignitor system. Triethylborane is a pyrophoric liquid with a high flame speed. Ignition of the engine was accomplished by supplying a mixture of fuel and air at a ratio of 0.04 to the combustor. The triethylborane was then forced with nitrogen under pressure into the recirculation zone area of the can until the fuel-air mixture ignited and sustained combustion.

6. BASELINE DESIGN

Photographs of the final design and fabricated low cost can flameholder and shroud are shown in Figures 12 and 13. All the material used in the design was either 321 stainless steel sheet or 321 stainless steel stock. The 321 stainless steel was used because of its excellent yield strength characteristics at high temperature. The can was fabricated from 0.050-inch thick stainless steel sheet. The holes were

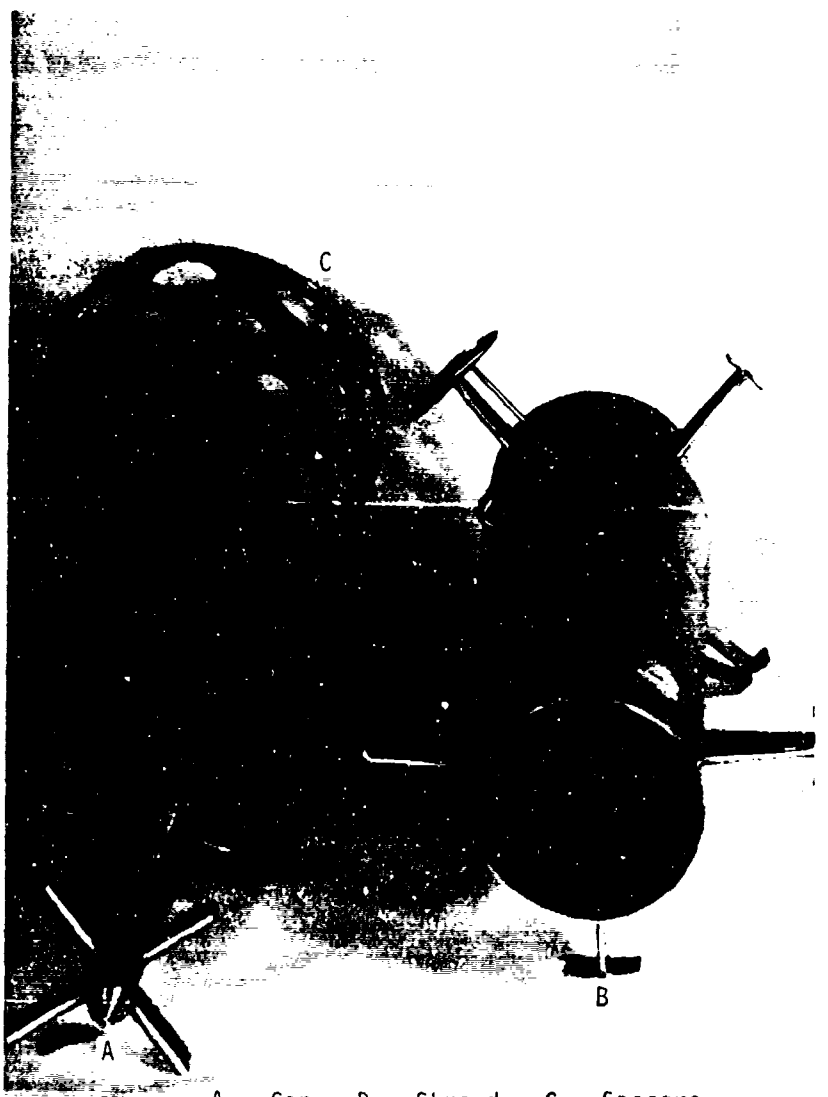

A - Can B - Shroud C - Spacers

Figure 12. Can Flameholder and Shroud

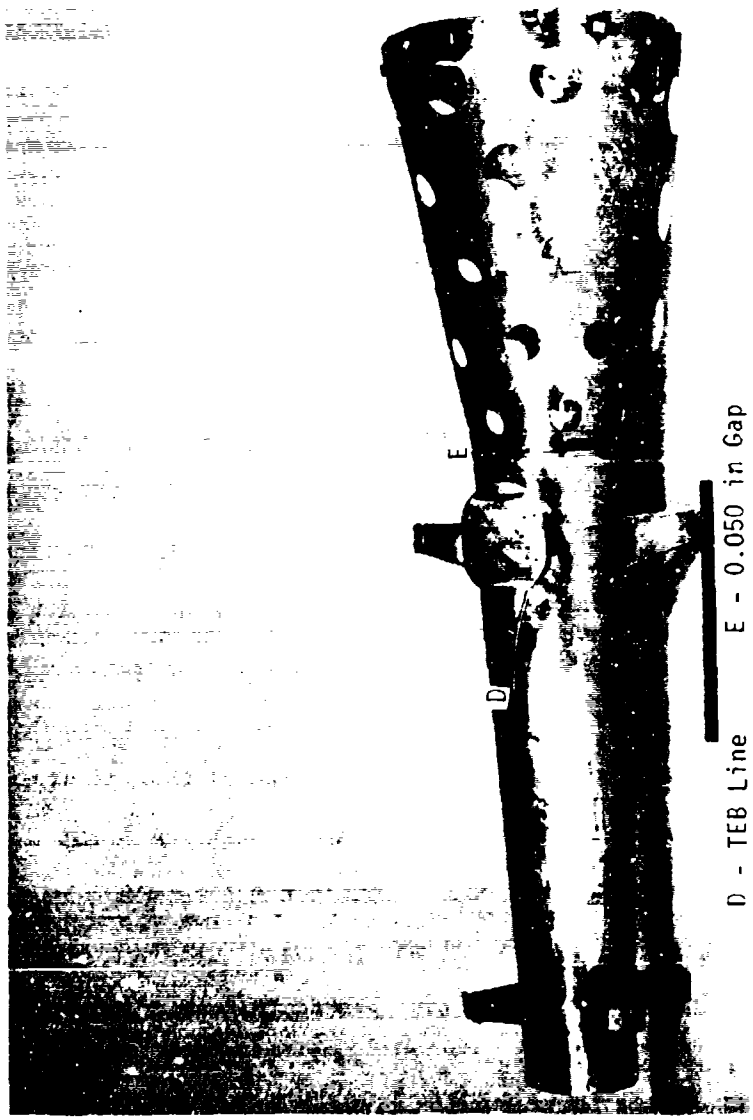

Figure 13. Can Flameholder and Shroud

punched in the sheets and the sheets were then rolled and seam welded. The shroud was also rolled from a 0.050-inch thick stainless steel sheet. The struts on the shroud, fabricated from two sections of sheet material, provided support from the engine wall. Eight struts of solid stock stainless steel supplied support for the flameholder to the shroud. These struts were upstream of the combustion and remained at ambient temperature. The can flameholder was not secured at the downstream end (base of the cone). Instead, the diameter of the base of the cone was less than the engine tailpipe diameter. The difference was made up with 12 spacers. This allowed the flameholder to freely move in the axial and radial direction with thermal growth during combustion. The axial growth due to thermal expansion was calculated to be 0.374 inch. The most severe thermal growth problem is at the downstream end of the shroud which is near the hot pilot flameholder wall. The shroud is near ambient temperature due to the cool, unburned fuel-air mixture flowing on the internal and external surface. The pilot can wall is at high temperature due to the combustion process. The radial thermal expansion of the pilot can at this station was calculated to be 0.042 inch; therefore, the combustor designed allowed a 0.050-inch gap between the shroud wall and the pilot can wall. This allowed the pilot can to expand radially without being restrained by the shroud, thus avoiding the chance of buckling of the pilot can.

The design was successful in achieving low cost. The total cost of the can combustor was $2468; this included $500 for material and fabrication labor costs of $1968.

SECTION III

EXPERIMENTAL TESTS AND PROCEDURES

1. TEST OUTLINE AND TEST CONDITIONS

The major objective of the tests was to optimize the combustion efficiency of the designed can combustor by varying the position and type of fuel injectors. Once this was accomplished, the combustion efficiency, stability characteristics, and the engine thrust were measured at the intersection of the Mach number and altitude boundaries of the flight envelope of Figure 2. The test conditions to simulate these four flight envelope points are given in Table IV.

The main fuel injector positions could be varied in the radial direction by sliding the fuel injectors in or out as previously shown in Figure 10. The radial position of the injectors was measured as the distance from the engine wall to the injector spray hole. The pilot injector was not varied in position but was varied in type. The two types tested were the hollow-cone nozzle and the full-cone nozzle, as previously shown in Figure 11.

Another variable was the pilot injector fuel flow setting. It was expected that the pilot flameholder would have an optimum fuel flow setting which would provide the maximum combustion efficiency. The combustion efficiency optimization tests were to be done at the 30,000 feet altitude conditions since these would be the most severe due to lower pressure. A test outline is shown in Table V.

TABLE IV

TEST CONDITIONS COMPUTED FOR STANDARD DAY
(59°F at Sea Level)

M_o	ALT(ft)	P_{ALT}(psia)	P_{T_1}(psia)	T_{ALT}(°R)	T_{T_1}(°R)	T_{T_1}(°F)
.7	20,000	6.732	9.338	447.4	491.2	31.2
.9	20,000	6.732	11.385	447.4	519.8	59.8
.7	30,000	4.356	6.042	411.8	452.2	-7.8
.9	30,000	4.356	7.367	411.8	478.5	18.5

TABLE V

TEST OUTLINE

Test	Objective	Variables	Conditions
1	Check test facility and instrumentation.	None	M_o = .7 Alt 20K
2	Optimize combustion efficiency. Check combustion stability.	Main fuel injector positions: 1.5, 2.0, and 2.5 inches.	M_o = .7 Alt 30K M_o = .9 Alt 30K
3	Optimize combustion efficiency. Check combustion stability.	Pilot fuel injector type 1. Hollow cone 2. Full cone	M_o = .7 Alt 30K M_o = .9 Alt 30K
4	Optimize combustion efficiency. Check combustion stability.	Pilot can fuel-air ratio	M_o = .7 Alt 30K M_o = .9 Alt 30K
5	Measure combustor efficiency at the intersection points of the flight envelope with best fuel injector configuration.	Altitude Mach number	M_o = .7 Alt 20K & 30K M_o = .9 Alt 20K & 30K

2. TEST INSTALLATION

The experimental tests were conducted in the Air Force Aero Propulsion Laboratory Ramjet Test Facility at Wright-Patterson AFB, Ohio. The test equipment is shown in Figure 14. The engine tailpipe section was installed in a cabin which was connected to exhausters which provided back pressures representative of altitude conditions. The inlet of the engine was connected to outside ambient air through a 12-inch diameter pipe. A total pressure rake, designed to ASME standards, was placed in the inlet of the engine and at the exit of the tailpipe. The total pressure associated with the flight Mach number being simulated was set at the inlet total pressure rake. This was done with a pneumatically controlled butterfly valve placed 28 feet upstream of the engine inlet. A subsonic flange tap orifice was used to measure engine air flow. The orifice was placed in relation with the valve and a set of flow straighteners in accordance with ASME standard such that the velocity gradient created by the valve would not affect air flow measurement accuracy. The bellows were installed to allow expansion of the pipe installation.

The tests were conducted by setting the cabin pressure and the engine inlet total pressure to the appropriate P_{ALT} and P_{T_1} for the required Mach numbers and altitude simulation. While there was no means of conditioning the air for correct temperature, testing during the winter months provided air near the desired value. The normal test sequence was to start taking data at low fuel flow rates to the engine and then increase the main fuel flow until rich flame blow-off occurred. The P_{T_1} and P_{ALT} values were corrected after each fuel flow setting to maintain correct Mach number and altitude. Pressure, temperature, and

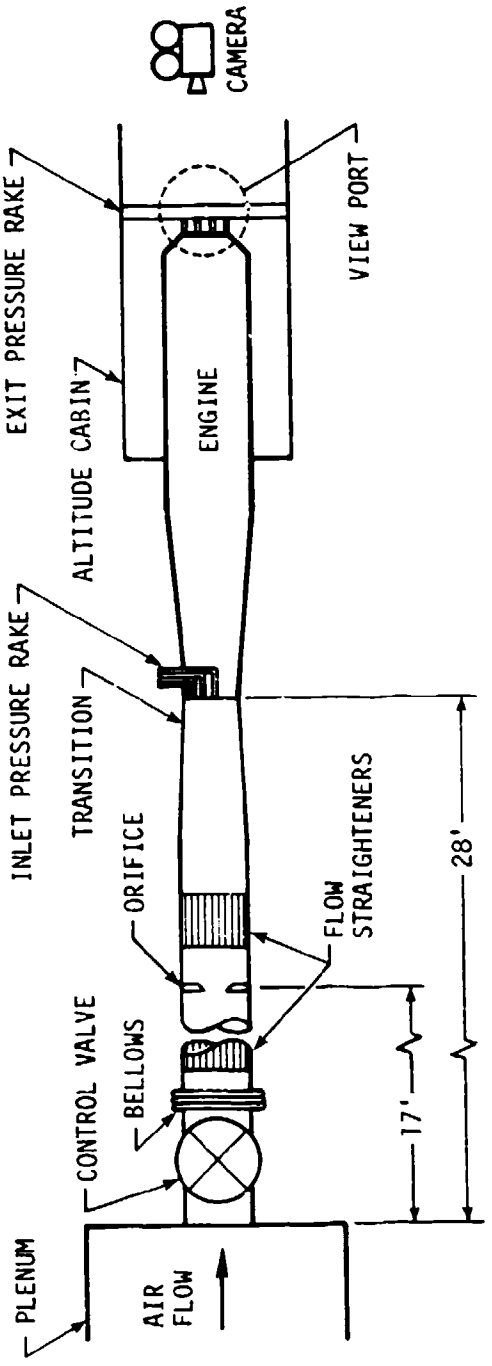

Figure 14. Subsonic Ramjet Test Set-up Schematic

fuel flow data were recorded at each fuel flow setting. The results were then translated into combustion efficiency and engine thrust as a function of fuel-air ratio for each fuel injector configuration at a given Mach number and altitude.

3. INSTRUMENTATION

The engine was instrumented for temperature and pressure measurements to calculate combustion efficiency and engine thrust. Temperatures were measured with thermocouples and pressures with transducers. Fuel flow was measured with a rotometer and a frequency converter. The analog signals from the thermocouples, transducers, and frequency converters were all recorded on a magnetic tape with the use of a data acquisition system. The magnetic tape was run in conjunction with a computer program which contained the required calibration data to change the recorded voltage signals to engineering units. Table VI gives a list of the parameters measured and Figure 15 shows the instrumentation locations.

Four total pressure pitot tubes were placed at the engine inlet, the diffuser exit, and the engine exit. At each station the four total pressures were averaged. The inlet total temperature was measured with the average of three total temperature probes. The tailpipe exit nozzle was instrumented with four thermocouples which were averaged.

Real-time color movies were taken from behind the engine looking into the combustion chamber. A telescopic lens was used which enabled zones of flameholding to be clearly distinguished. The lens was used either with the movie camera or for direct visual observation.

TABLE VI

INSTRUMENTATION LIST

Parameter	Averages	Description	Location
P_{10}		Flange Tap Pressure, Top	Orifice, Upstream
P_{20}		"	Orifice, Downstream
P_{30}		Flange Tap Pressure, Bottom	Orifice, Upstream
P_{40}		"	Orifice, Downstream
P_{101}		Inlet Static Pressure	Engine Inlet
P_{102}	P_1	"	"
P_{103}		"	"
P_{104}			
P_{111}		Inlet Total Pressure	Engine Inlet
P_{112}	P_{T_1}	"	"
P_{113}		"	"
P_{114}			
P_{121}		Diffuser Static Pressure	Diffuser Exit
P_{122}	P_2	"	"
P_{123}		"	"
P_{124}			
P_{131}		Diffuser Total Pressure	"
P_{132}	P_{T_2}	"	"
P_{133}		"	"
P_{134}			
P_{141}		Combustor Static Pressure	Combustor Wall
P_{142}		"	"
P_{161}		Exit Static Pressure	Exit Nozzle
P_{162}	P_5	"	"
P_{163}		"	"
P_{164}			
P_{171}		Exit Total Pressure	"
P_{172}	P_{T_5}	"	"
P_{173}		"	"
P_{174}			
P_{191}	P_{ALT}	Altitude Pressure	Cabin Wall
P_{193}		"	"
T_o		Ambient Air Temperature	
$T_{T_{21}}$		Total Temperature	Inlet
$T_{T_{22}}$	T_{T_1}	"	"
T_{23}		"	"
T_{81}		Nozzle Wall Temperature	Exit Nozzle Ring
T_{82}	T_{EXIT}	"	"
T_{83}		"	"
T_{84}		"	"
$\dot{W}_F$		Main Fuel Flow	
$\dot{W}_{F_M}$		Pilot Fuel Flow	
$\dot{W}_{F_P}$			

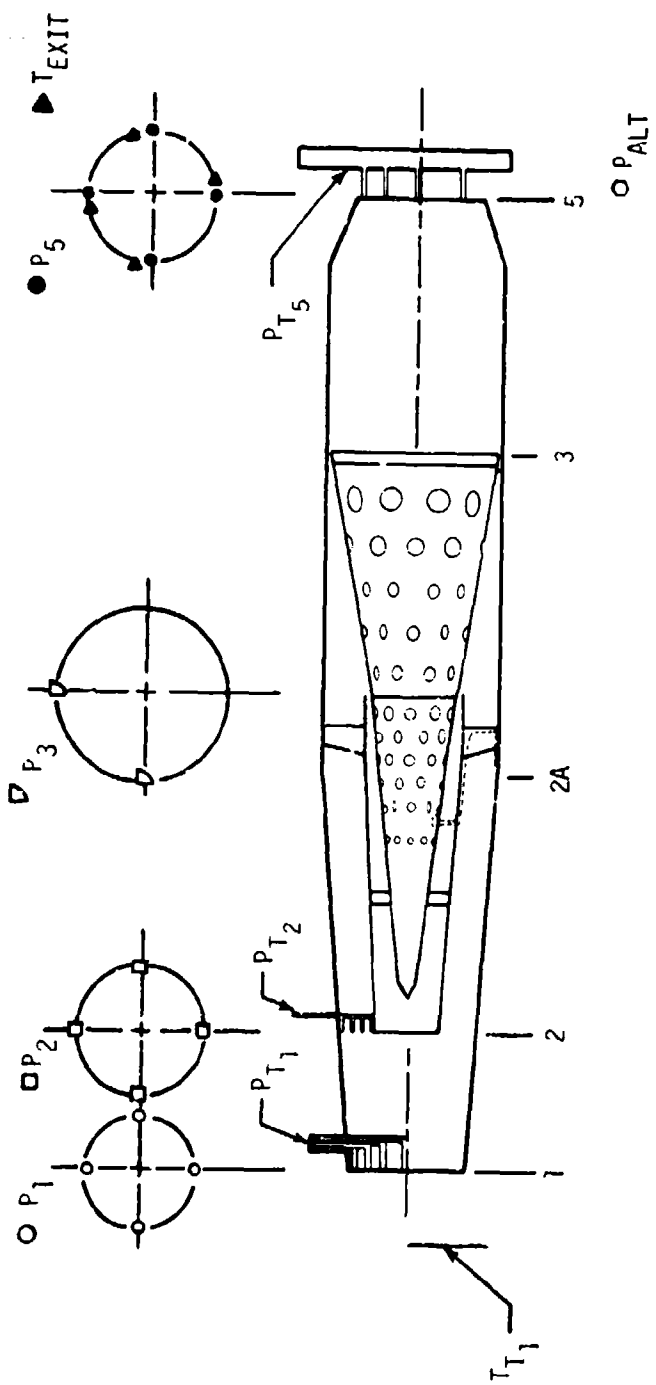

Figure 15. Instrumentation Locations

4. DATA REDUCTION AND CALCULATION METHODS

A computer program, LOWCOST 2, was written to perform the engine performance calculations using the measured engine pressure and temperature data of Table VI. The performance calculations are discussed below.

The engine air flow, $\dot{W}_{A_T}$, is calculated using the pressures P_{10}, P_{20}, P_{30}, and P_{40} of the orifice plate. Next, the Mach number at engine Station 1 (see Figure 15 for engine station nomenclature) is calculated from

$$M_1 = \left\{ \frac{2}{\gamma_1 - 1} \left[\left(\frac{P_{T_1}}{P_1} \right)^{\frac{\gamma_1 - 1}{\gamma_1}} - 1 \right] \right\}^{1/2} \qquad (1)$$

In this expression P_{T_1} and P_1 have values obtained through measurements. The ratio of specific heats $\gamma_1 = 1.4$.

The division of the air flow to the main and pilot flameholders is calculated next. The air flow to the main flameholder is calculated using the measured conditions at engine Station 2. For an ideal gas, the rate of mass flow

$$\dot{W}_A = \rho A V \qquad (2)$$

can be rearranged to yield

$$\dot{W}_A = PAM\sqrt{\frac{g\gamma}{RT}} \tag{3}$$

where $M = V/\sqrt{g\gamma RT}$ is the Mach number.

Using

$$\frac{T_T}{T} = 1 + \frac{\gamma - 1}{2} M^2 \tag{4}$$

the value of T can be found and substituting it into Equation (3) gives

$$\dot{W}_A = PAMg\sqrt{\frac{\gamma}{gRT_T}} \left[1 + \frac{\gamma - 1}{2} M^2\right]^{1/2} \tag{5}$$

Now defining

$$\mathring{m} = g\sqrt{\frac{\gamma}{gR}}\ M \left[1 + \frac{\gamma - 1}{2} M^2\right]^{1/2} \tag{6}$$

the mass flow relation becomes

$$\dot{W}_A = PA\mathring{m}\sqrt{T_T} \tag{7}$$

It is this form in which mass flow rate will be most useful in the data reduction calculations.

From Equation (7), the main flameholder air flow is given by

$$\dot{W}_{A_M} = P_2 A_2 \mathring{m}_2 \Big/ \sqrt{T_{T_2}} \tag{8}$$

where P_2 is obtained by measurement, $\mathring{m}_2$ is calculated from $M_2 = f(P_{T_2}/P_2)$ and Equation (6), T_{T_2} is assumed equal to T_{T_1} which is measured, and A_2 has a value of 68.666 in^2.

The pilot flameholder air flow is given by the conservation of mass relation

$$\dot{W}_{A_P} = \dot{W}_{A_T} - \dot{W}_{A_M} \tag{9}$$

The fuel-air ratios are now calculated using the measured fuel flows

$$\left(\frac{f}{a}\right)_T = \frac{\dot{W}_{F_M} + \dot{W}_{F_P}}{\dot{W}_{A_T}} \tag{10}$$

$$\left(\frac{f}{a}\right)_M = \frac{\dot{W}_{F_M}}{\dot{W}_{A_M}} \tag{11}$$

$$\left(\frac{f}{a}\right)_P = \frac{\dot{W}_{F_P}}{\dot{W}_{A_P}} \tag{12}$$

Next the conditions at engine Station 5 are calculated. In these calculations the real gas thermodynamic properties after combustion were used. Figures 16, 17 and 18 show the ideal temperature rise (ΔT_{T_I}), the molecular weight (MW_5), and the ratio of specific heats (γ_5) for the combustion products. The nozzle exit Mach number is given by

$$M_5 = \left\{ \frac{2}{\gamma_5 - 1} \left[\left(\frac{P_{T_5}}{P_5} \right)^{\frac{\gamma_5 - 1}{\gamma_5}} - 1 \right] \right\}^{1/2} \tag{13}$$

where P_{T_5} and P_5 have been measured and γ_5 is obtained from Figure 18. The nozzle exit total temperature can be calculated using the mass flow relation at Station 5, which is

$$\dot{W}_5 = P_5 A_5 C_{N_D} \mathring{m}_5 \Big/ \sqrt{T_{T_5}} \tag{14}$$

Or rearranging

$$T_{T_5} = \left[\frac{P_5 A_5 C_{N_D} \mathring{m}_5}{\dot{W}_5} \right]^2 \tag{15}$$

where P_5 is obtained by measurement, A_5 has the value of 108.99 in^2, $\mathring{m}_5$ is calculated from M_5 using Equation (6), $\dot{W}_5$ is the sum of $\dot{W}_{A_T}$ and $\dot{W}_{F_T}$, and C_{N_D} is the nozzle discharge coefficient which was found experimentally and is presented in Figure 19.

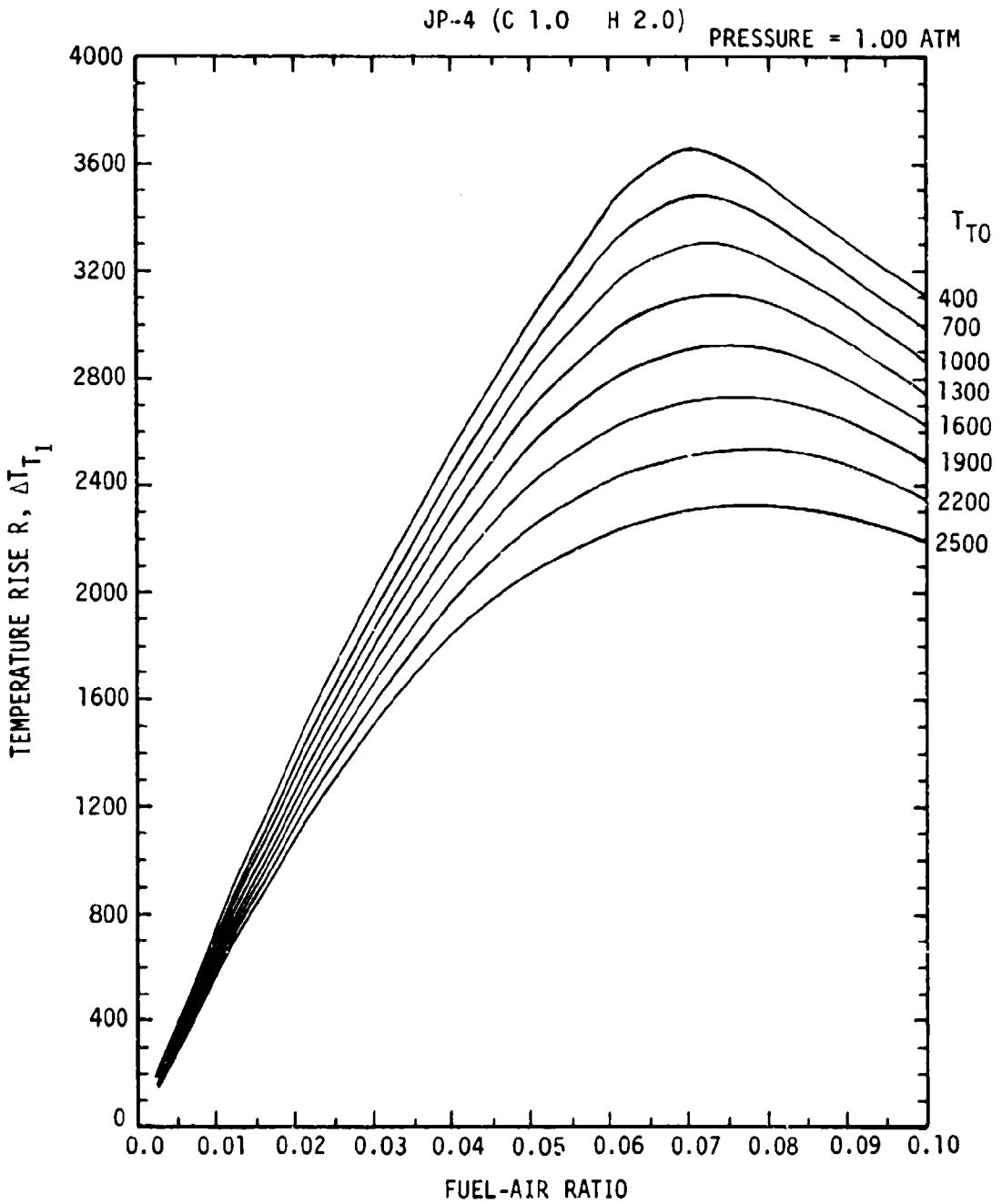

Figure 16. Ideal Temperature Rise for Given Fuel-Air Ratio and Inlet Temperature

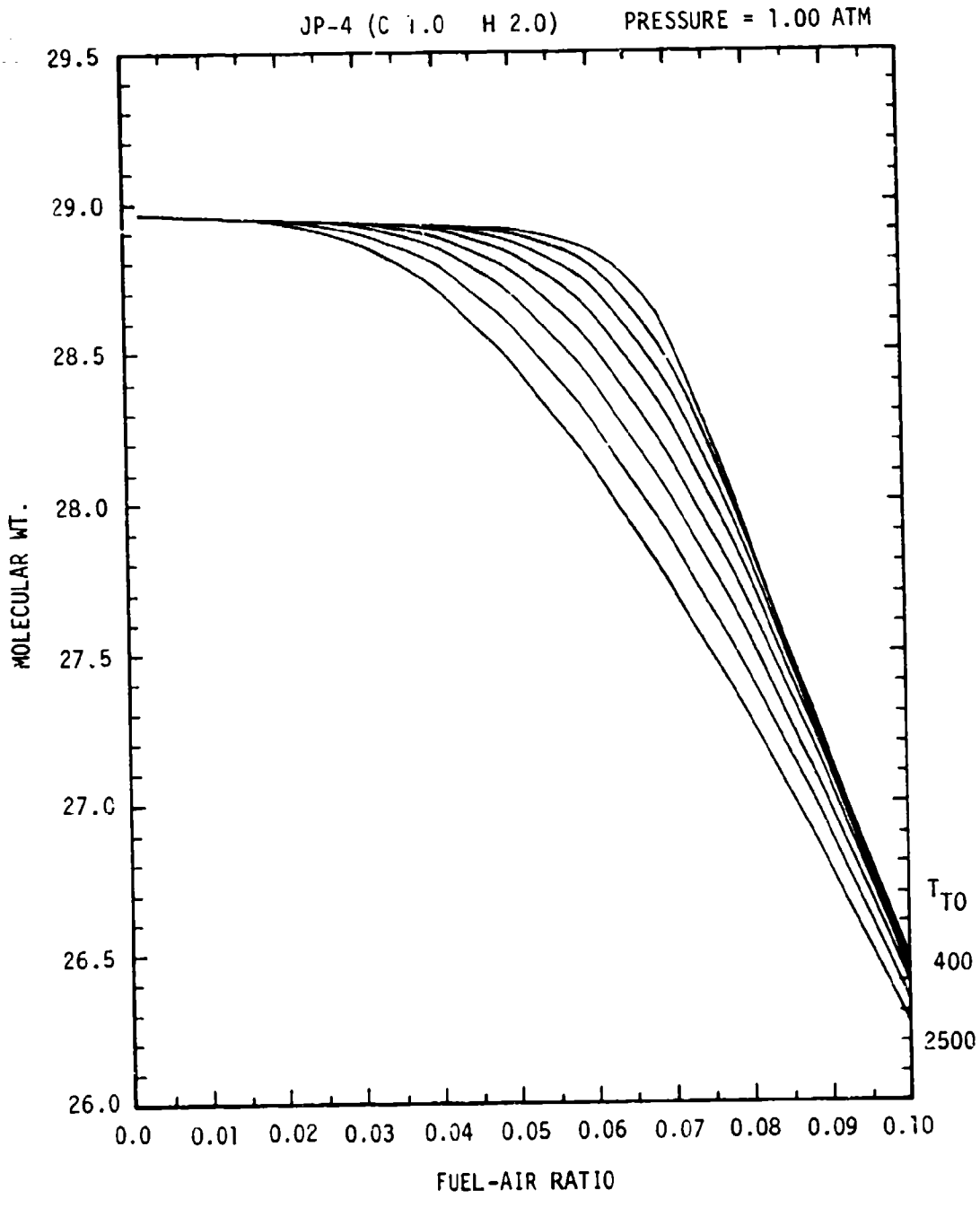

Figure 17. Molecular Weight of Combustion Products for Given Fuel-Air Ratio and Inlet Temperature

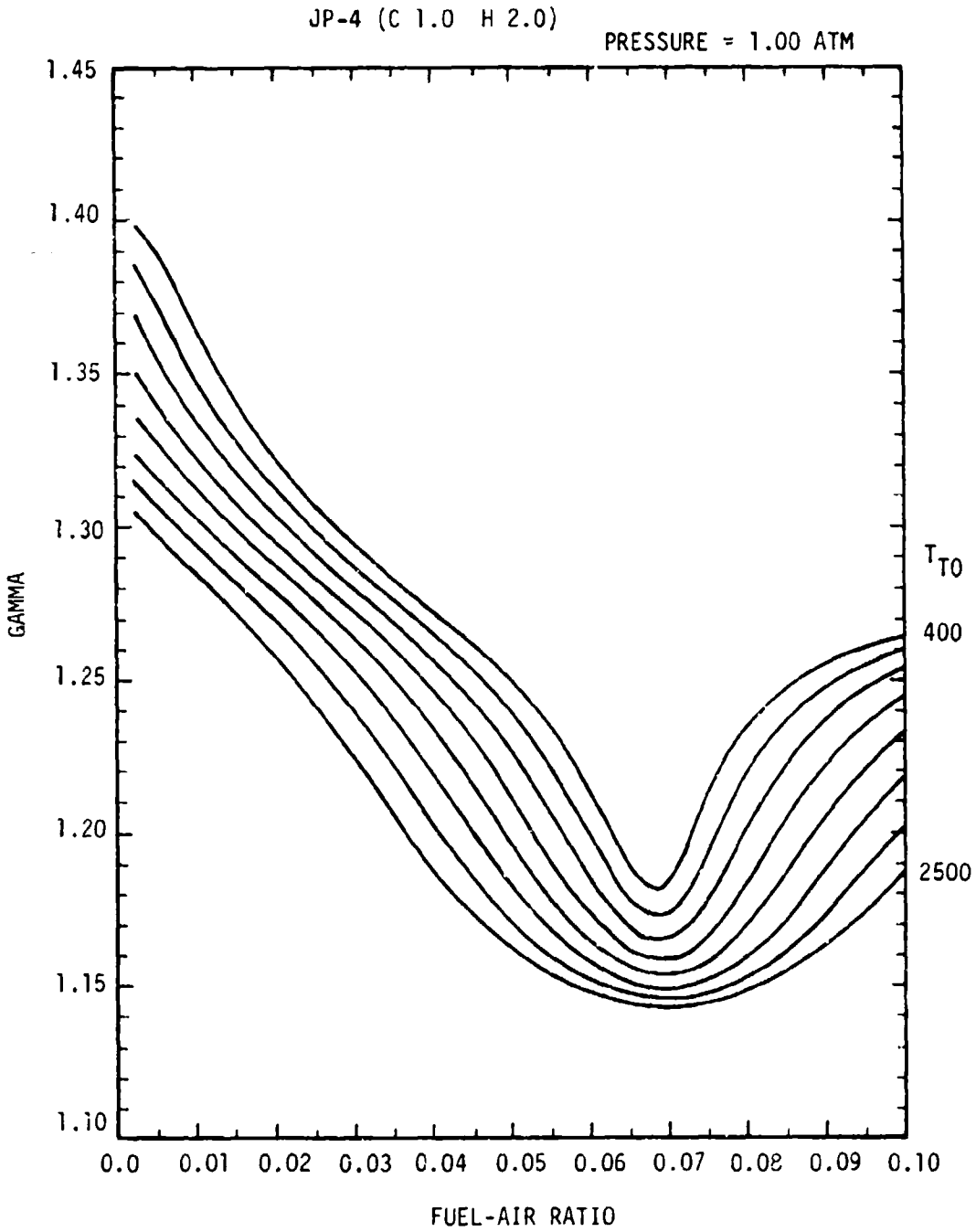

Figure 18. Ratio of Specific Heats of Combustion Products for Given Fuel-Air Ratio and Inlet Temperature

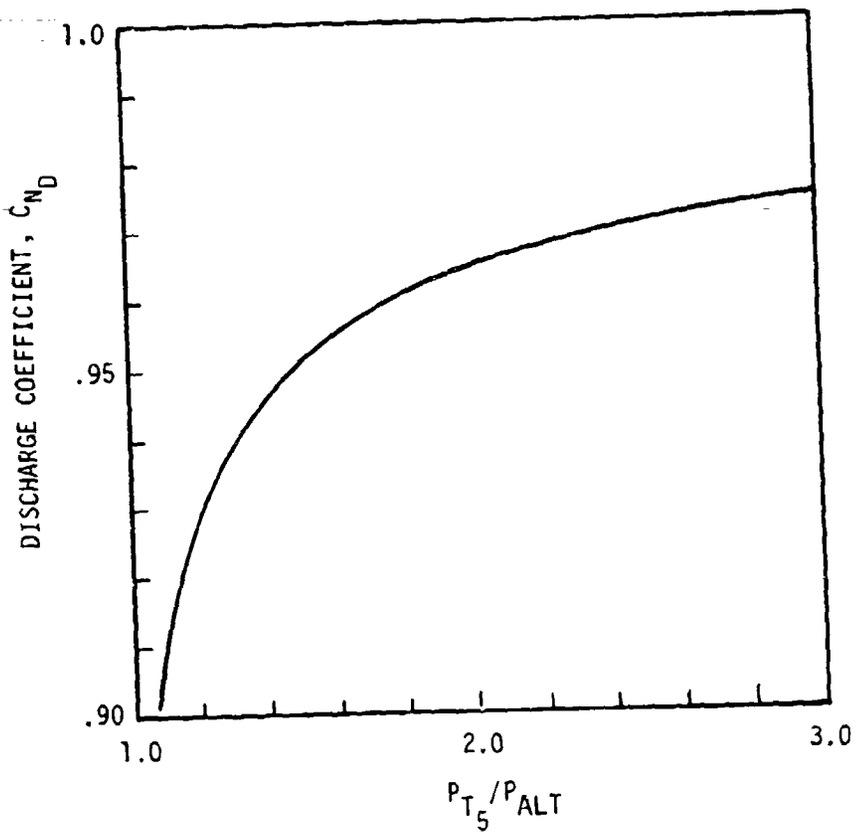

Figure 19. Exit Nozzle Discharge Coefficient

The thermal combustion efficiency is now defined as

$$n_c = \frac{T_{T_5} - T_{T_1}}{\Delta T_{T_I}} \tag{16}$$

where ΔT_{T_I} is from Figure 16, T_{T_1} is measured and T_{T_5} is Equation (15).

Thrust performance for ramjet engines is normally presented as net jet thrust, which is calculated on the control volume from Station 0 to Station 5. In these tests, the freestream Mach number, M_o, is being simulated by setting the correct total pressure at Station 1. In order that the test data can be compared to other results, the simulated freestream M_o and A_o will be calculated. The simulated freestream Mach number is given by

$$M_o = \left\{ \frac{2}{\gamma_1 - 1} \left[\left(\frac{P_{T_o}}{P_{ALT}} \right)^{\frac{\gamma_1 - 1}{\gamma_1}} - 1 \right] \right\}^{1/2} \tag{17}$$

which assumes $P_{T_o} = P_{T_1}$.

The simulated area of the air flow stream at Station 0 can be found using mass conservation

$$\dot{W}_{A_o} = \dot{W}_{A_1}$$

Therefore, using Equation (7) and assuming $P_{T_0} = P_{T_1}$ and $T_{T_0} = T_{T_1}$, the capture area ratio is given by

$$\frac{A_0}{A_1} = \frac{\dot{m}_1 P_1}{\dot{m}_0 P_{ALT}} \tag{18}$$

where P_1 and P_{ALT} are obtained by measurement, $\dot{m}_1$ is calculated from M_1 using Equation (6), $\dot{m}_0$ from M_0 using Equation (6), and A_1 has a value of 62.072 in^2.

The net jet thrust is given by

$$F_{NJ} = P_5 A_5 \eta_D \left(1 + \gamma_5 M_5^2\right) - P_{ALT} A_0 \left(1 + \gamma_0 M_0^2\right) - P_{ALT}\left(A_5 - A_0\right) \tag{19}$$

where P_5 and P_{ALT} are obtained by measurement, A_5 has the value of 108.99 in^2, γ_0 has the value of 1.4, γ_5 is obtained from Figure 18, M_5 is Equation (13), M_0 is Equation (17), A_0 is Equation (18), and η_D is the nozzle discharge efficiency with a value of 0.98.

In order to present thrust performance as dimensionless, the thrust coefficient, C_F, is defined as

$$C_F = \frac{F_{NJ}}{\frac{1}{2} \gamma_0 P_{ALT} A_3 M_0^2}$$

where F_{NJ} is Equation (19), γ_0 has the value of 1.4, P_{ALT} is obtained by measurement, A_3 has the value of 167.7 in^2, and M_0 is Equation (17).

Another important ramjet performance parameter is the specific fuel consumption which is the measure of lb_m of fuel used per hour per lb_f of thrust and is defined as

$$SFC = \frac{\dot{W}_{F_T}}{F_{NJ}}$$

SECTION IV

TEST RESULTS

1. SUMMARY

During the test program, 36 hours of combustor operation time were totaled. The same hardware was used throughout the test program with no hardware failures. The initial test of Table V, Test Outline, was a cold flow run without combustion at the Mach 0.7, altitude 20,000 feet condition. This test was made to check the facility and instrumentation. The main result of the initial test was the establishment of the fact that the air flow pressure and velocity supplied to the engine inlet did not vary with radial position in the pipe. The next three tests of Table V were to be fuel injector variations to optimize combustion efficiency at the most severe conditions, which were the Mach 0.7 and 0.9, altitude 30,000 feet conditions. However, attempts to run the can at the 30,000 feet test conditions failed because combustion could not be sustained. To achieve stable combustion at these conditions, some design changes would be necessary. Before making these changes, however, the combustion efficiency optimization tests were conducted at the 20,000 feet altitude condition, since the combustor would operate smoothly at this condition. With this experience, an optimum fuel injector system could be used when attempts would be made at the 30,000 feet test conditions. The results of the combustion efficiency optimization Tests 2, 3, and 4 are given in Section IV.2.

Between Test 4 and Test 5 of Table V, an experimental design change program was undertaken. The design program consisted of a blow-off data

correlation study of the pilot can, two pilot can design changes, and experimental verification of the design changes. The above design changes resulted in successful operation of the can at the 30,000 feet test conditions. These design changes are discussed in Section IV.3.

Once the design changes were complete, Test 5 was conducted which was the measuring of the combustor performance at the test conditions of Mach 0.7 and 0.9, altitude 20,000 feet and 30,000 feet. The results of Test 5 are discussed in detail in Section IV.4.

In order to check the validity of the test results, the actual ramjet performance was compared to model ramjet performance which was obtained with a methematical model. This comparison is discussed and shown graphically in Section IV.5.

2. TESTS FOR COMBUSTION EFFICIENCY OPTIMIZATION

After the can is designed and constructed with a fixed number of stages, a fixed number of holes per stage, and fixed hole diameters, the only design variable left is the fuel injection system. The distribution of the fuel to the combustor greatly influences the combustion efficiency in that the fuel must be distributed so there is not more fuel present in any stage of the combustor than can be burned. Also, the method of fuel injection of the fuel affects the vaporization of the fuel in the air stream and therefore affects the reaction time necessary to complete the combustion process. The best method for obtaining a good fuel injection system is by experiment. The variables of the fuel system are the main fuel injector position (radial distance from the engine wall to

the spray hole), the pilot fuel nozzle type, and the pilot can fuel-air ratio. The objective of the combustion efficiency optimization tests was to exercise the above variables independently to obtain the maximum combustion efficiency. The optimization tests were conducted at the Mach 0.7 and 0.9, altitude 20,000 feet engine operating conditions.

a. Effect of Main Fuel Injector Position

The main fuel injectors must provide a near homogeneous mixture to the main can. For the highest combustion efficiency, the main fuel injectors must not allow the local fuel-air ratio in any of the recirculation zones to become greater than stoichiometric. The variable of the main fuel injector design was the radial distance of the spray hole from the engine wall, as shown previously in Figure 10. Three distances were tested: 2.5 inches, 2.0 inches, and 1.5 inches. The 2.5-inch distance was as far as the injectors could be positioned without interfering with the pilot can shroud. As shown by Figure 20, the 2.5-inch position provided the best combustion efficiency throughout the total engine fuel-air traverse for the Mach 0.7, altitude 20,000 feet test condition. Similar results were obtained at the Mach 0.9, altitude 20,000 feet test condition, as shown in Figure 21. The 1.5-inch position was not tested at the Mach 0.9, altitude 20,000 feet condition since the trend of poorer combustion efficiency with less injector distance was being repeated.

To substantiate the results of Figures 20 and 21, the color movies and visual observation showed more traces of red fuel-rich burning taking place outside of the engine tailpipe as the fuel injectors were brought closer to the wall. Fuel burning outside of the engine in

MACH NUMBER - 0.7

ALTITUDE - 20K

FULL-CONE PILOT NOZZLE - 400 lb_m/hr FLOW RATE

FUEL - JP-4

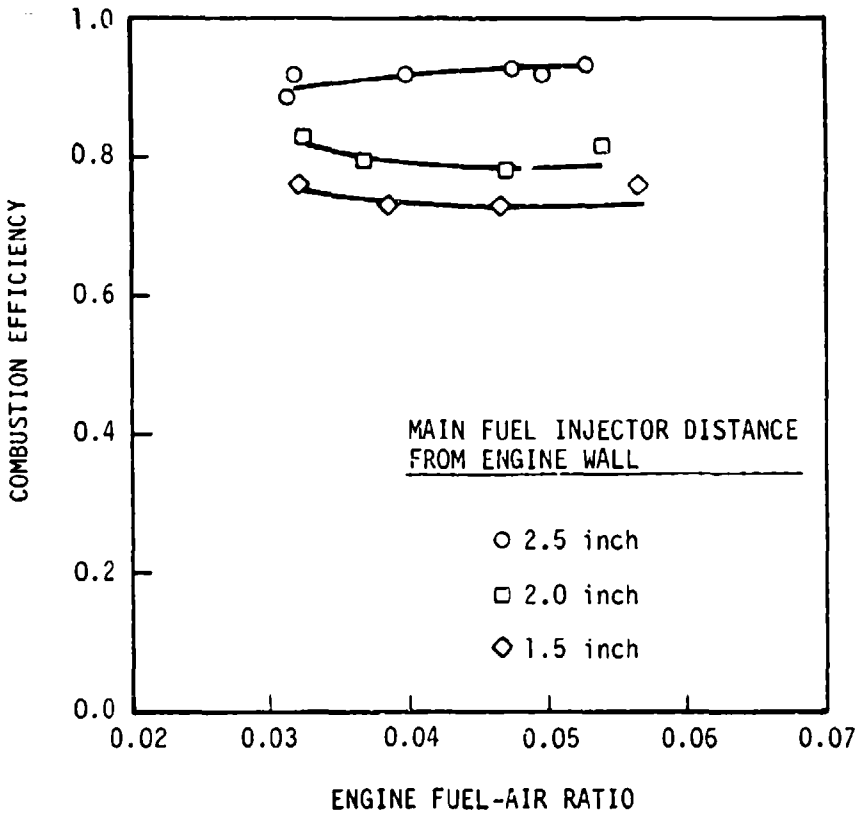

Figure 20. Effect of Main Fuel Injector Position

MACH NUMBER - 0.9

ALTITUDE - 20K

FULL-CONE PILOT NOZZLE - 500 lb_m/hr FLOW RATE

FUEL - JP-4

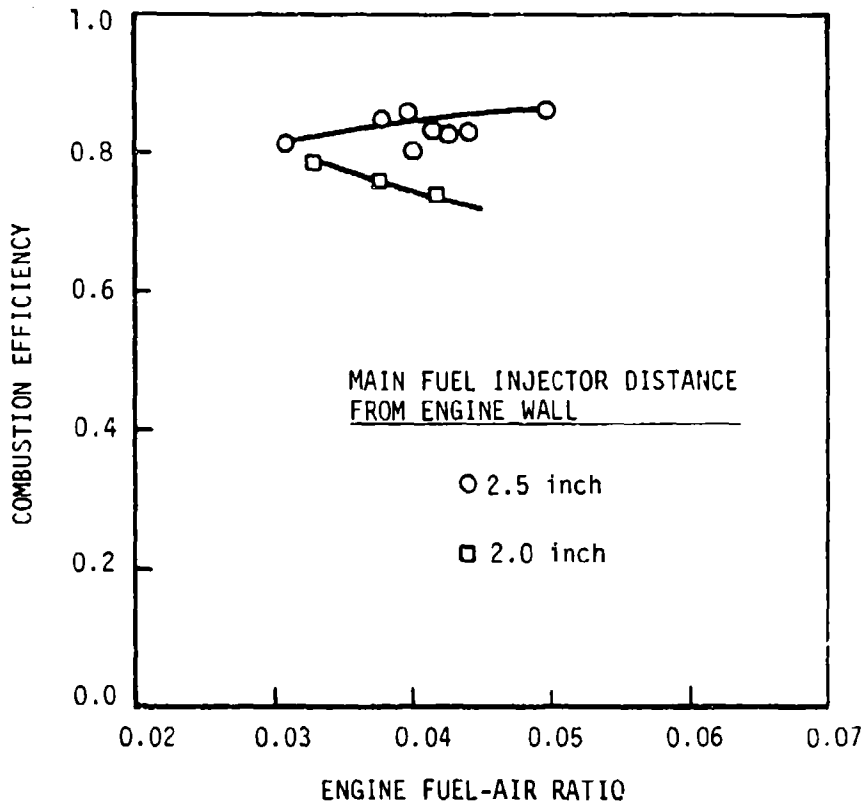

Figure 21. Effect of Main Fuel Injector Position

the exhaust plume naturally results in engine combustion efficiency loss. The probable cause of the 1.5- and 2.0-inch positions providing less combustion efficiency is that these two configurations provide more fuel to other radial main can hole stages. Because these stages are also nearer the exit nozzle, the recirculation zones behind these stages are shorter. Therefore, there is less time for complete combustion of all the fuel to take place.

Based on the above results, the 2.5-inch position for the main fuel injectors was used in all subsequent tests.

b. Effect of Pilot Fuel Nozzle Type

The pilot fuel nozzle must provide a near homogeneous mixture to the pilot can. Since the pilot fuel nozzle must spray in the small restricted area of the 5.5-inch diameter shroud, it is important that fuel not spray too far in the radial direction, causing the fuel flow to impinge on the shroud wall. This would result in a flowing liquid stream of fuel down the wall rather than a well-vaporized fuel-air mixture which in turn would result in lowered combustion efficiency.

As has been mentioned, two types of nozzles were tested and compared at the Mach 0.7, altitude 20,000 feet test condition. These were the hollow-cone and full-cone types. Figure 22 shows that better combustion efficiency was obtained with the full-cone nozzle throughout the total engine fuel-air ratio range. Also, during the tests, combustion instability was noted with the hollow-cone nozzle at the high fuel flow rates. The instability resulted in the flame blowing out on two

MACH NUMBER - 0.7

ALTITUDE - 20K

MAIN INJECTORS AT 2.5 INCH

PILOT FLOW RATE - 400 lb_m/hr

FUEL - JP-4

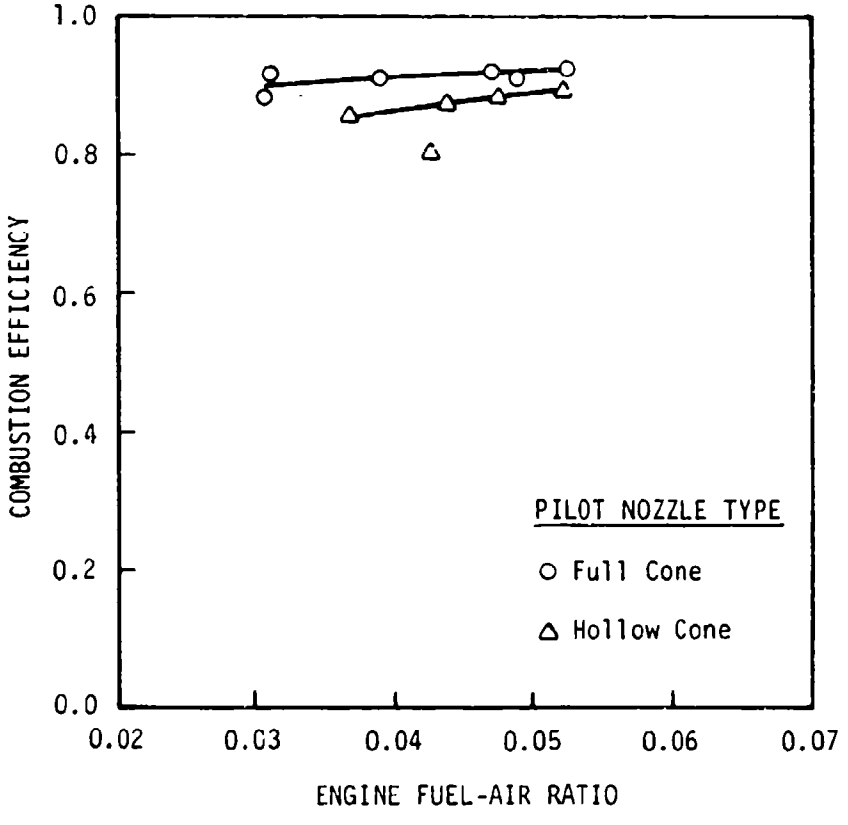

Figure 22. Effect of Pilot Fuel Injector Type

occasions. Since for the Mach 0.9, altitude 20,000 feet condition higher fuel flow rates would be required, the hollow-cone nozzle which previously resulted in an instability problem was not compared to the full-cone nozzle at Mach 0.9 test condition. The full-cone nozzle was used successfully at the Mach 0.9, 20,000 feet condition during the tests to determine the influence of main fuel injector position on combustion efficiency. Therefore, the full-cone nozzle was selected for subsequent tests also.

c. Effect of Pilot Fuel-Air Ratio

The effect on combustion efficiency by the variation of the pilot fuel-air ratio is shown in Figure 23 for the Mach 0.7, altitude 20,000 feet test condition. It would be expected that the maximum engine combustion efficiency would be achieved if the pilot can was operating near stoichiometric. This is shown to be true in Figure 23. This test was run by holding the pilot fuel flow constant at one of the three fuel settings (400, 350, and 500 lb/hr) while the main fuel flow was varied to change the overall engine fuel-air ratio. As the main fuel flow is increased, and thus the total engine fuel-air ratio increased, there is less air flow through the engine. Therefore, with the fixed pilot fuel flow and decreasing pilot air flow, the pilot fuel-air ratio also increases. The pilot fuel-air ratio range for the 400 lb/hr setting was 0.061 to 0.065, for the 350 lb/hr setting the range was 0.055 to 0.057, and for the 500 lb/hr setting the range was 0.073 to 0.079. As can be seen, the near stoichiometric pilot fuel-air ratio range of the 400 lb/hr fuel setting provided the best combustion efficiency over

MACH NUMBER - 0.7

ALTITUDE - 20K

MAIN INJECTORS AT 2.5 INCH

HOLLOW-CONE PILOT NOZZLE

FUEL - JP-4

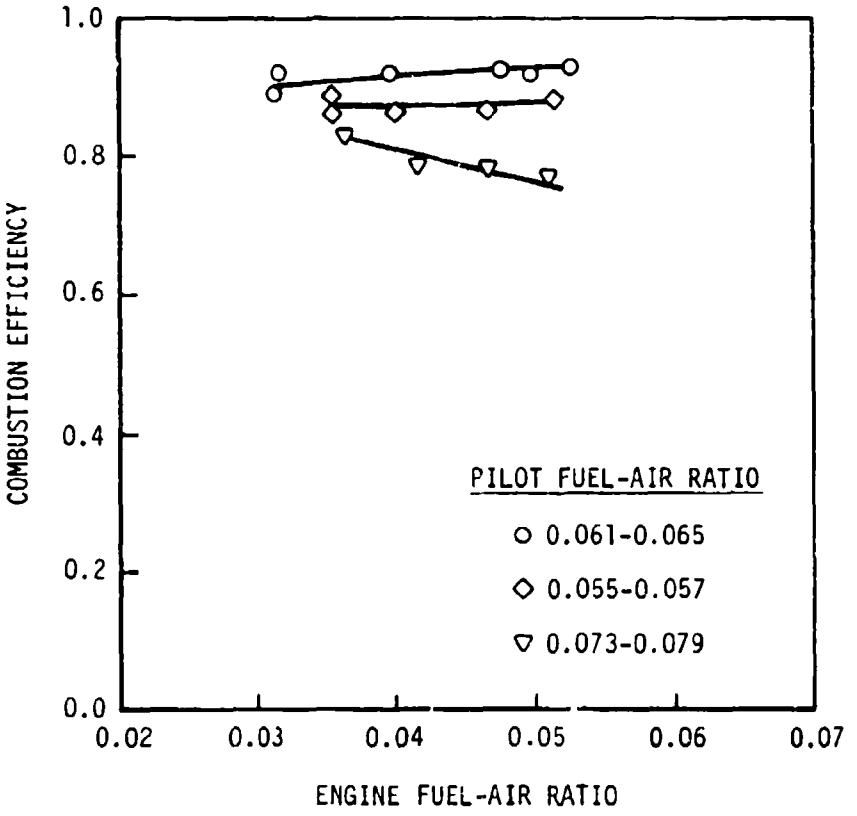

Figure 23. Effect of Pilot Fuel-Air Ratio

the entire range of total engine fuel-air ratios tested. The pilot fuel-air ratio was therefore set as near stoichiometric as possible for subsequent tests.

3. DESIGN CHANGES TO ACHIEVE COMBUSTOR OPERATION AT INCREASED ALTITUDE

Attempts to run the combustor at the 30,000 feet test conditions with the optimized fuel injection system resulted in combustion instability and flame blow-off. A stability limit curve of the altitude and fuel-air ratio region which would provide stable combustion is shown in Figure 24. This curve is for a constant Mach number of 0.7. Visual observation of the engine flame-outs showed that initial flame blow-off was occurring in the center of the engine which is the pilot can; therefore, a redesign of the pilot can was made.

a. Baseline Pilot Can Blow-off Data Correlation

A blow-off data correlation was made by operating the engine with the pilot can and pilot fuel injector only. The purpose of the test was to determine the effect of pilot combustor pressure, pilot air flow rate, and pilot fuel-air ratio on the blow-off limits of the pilot can. The range of variables was: pressure, 5.988 to 11.269 psia; air flow, 1.382 to 2.849 lb_{in}/sec; and fuel-air ratio, 0.048 to 0.119. The inlet total temperature for this test varied only slightly from 528.2 to 531.9°R. The blow-off limits were found by setting the pilot can pressure and pilot can air flow. The pilot fuel flow setting was then reduced until lean blow-off occurred. The combustor was then reignited and the pilot fuel flow setting was increased until rich blow-off occurred. The Longwell and Weiss correlation parameter without the recirculation zone volume term was used to correlate the data. The volume

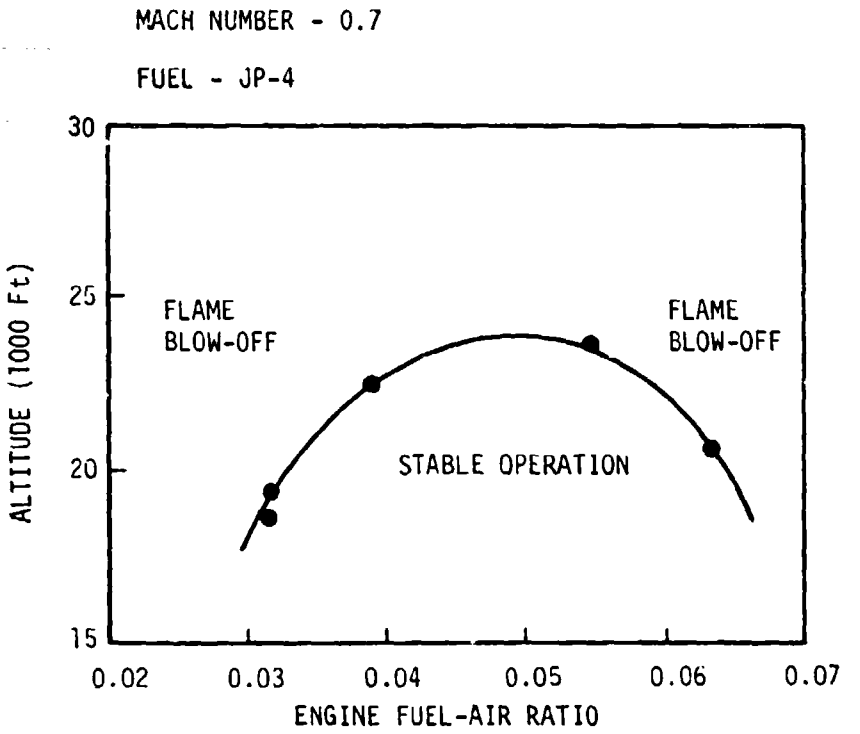

Figure 24. Stability Limits of Baseline Design

term was not included since it was fixed and therefore would not change and effect the blow-off limits. The result of the blow-off data correlation is shown in Figure 25. The parameter $\dot{W}_{A_P}$ is the pilot can air flow and P_2 is the pressure at the pilot can entrance. The significance of the pilot can blow-off correlation is that for a known pressure the air flow which will provide stable combustion in the pilot can flameholder can be found. The combustor entrance pressure representative of the Mach 0.7 and 0.9, altitude 30,000 feet test conditions was used with the correlation to find an air flow rate which would provide a correlation parameter value of 3.0, thus providing wide stable operating limits. This air flow rate was found to be lower than the pilot can air flow rates being provided by the baseline design. Therefore, a design change was necessary to reduce the pilot can air flow rate.

b. Combustor Design Changes

To reduce the pilot air flow an extension was added to the shroud which reduced the shroud inlet from a 5.5-inch diameter to a 3.0-inch diameter (Figure 26). The engine was tested with the shroud extension. The result was increased stable operation to an altitude condition of 27,000 feet, as shown in Figure 27. This still was not satisfactory. It was thought that with the lower pilot can air flow rates, the fuel-air mixture entering the first stage of holes was not penetrating into the pilot recirculation zone due to the lower velocities. A well-defined recirculation zone must be formed or stable flameholding cannot be achieved because there will not be a turbulent mixing region for the combustion to occur. Therefore, a set of air scoops was designed,

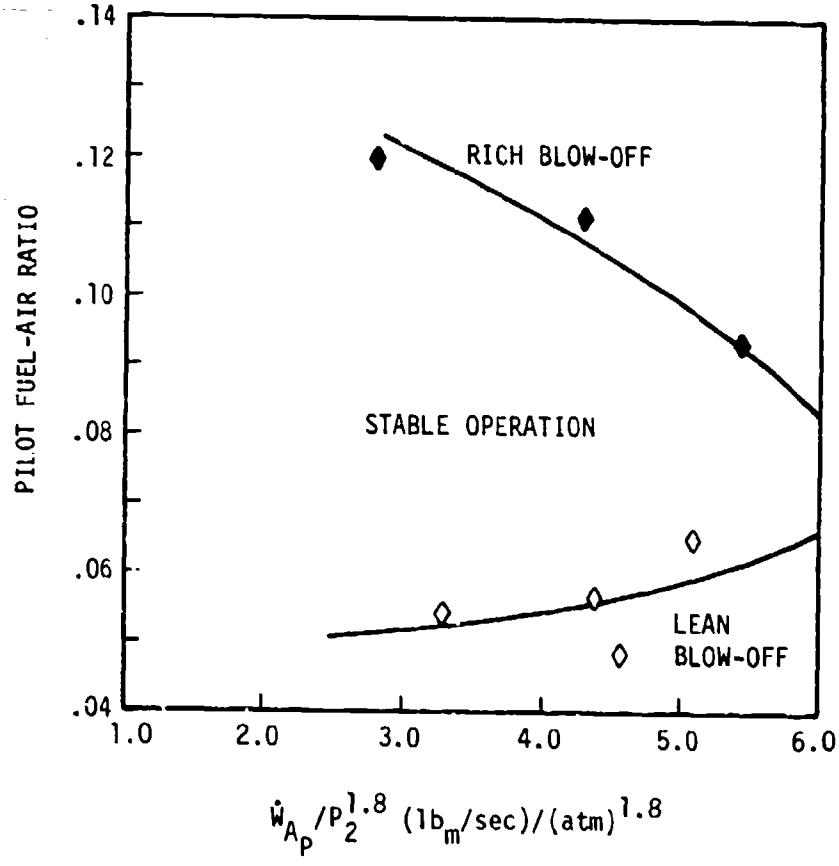

Figure 25. Pilot Can Blow-off Data Correlation

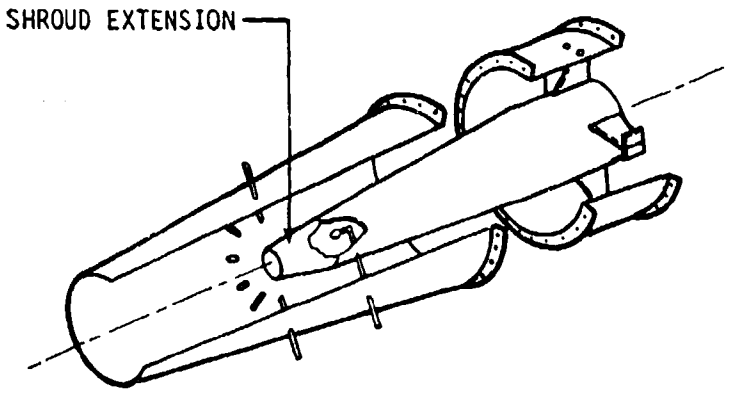

Figure 26. Shroud Extension

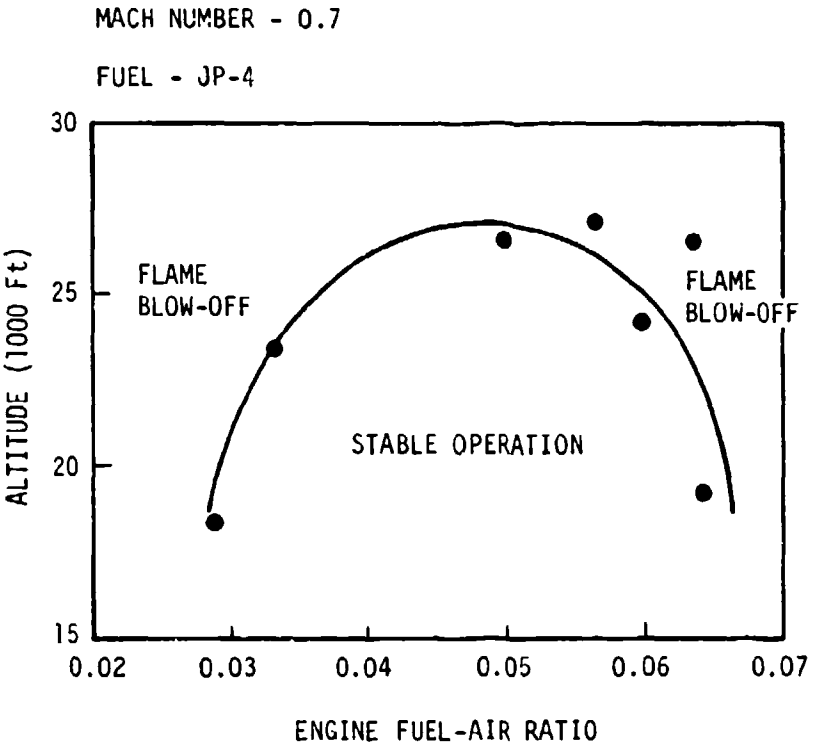

Figure 27. Stability Limits of Baseline Design with Shroud Extension

fabricated, and placed on the downstream side of the first stage of pilot can holes. The scoops shown in Figure 28 were 0.5 inch tall and 0.5 inch wide. The purpose of the air scoops was to help change the direction of the oncoming fuel-air mixture and force the mixture to penetrate and form a hot recirculation zone. The engine was then tested with the shroud extension and air scoops. The combination was successful in extending the stable operating region of the can combustor into the Mach 0.07, altitude 30,000 feet test condition, as shown in Figure 29. The condition of Mach 0.9, altitude 30,000 feet was not attainable, partially due to facility problems at this high Mach number and altitude. This condition was near the operating limit of the facility and the test conditions were difficult to set and stabilize. The changing test condition setting added to the instability of the combustor. Therefore, performance was taken at Mach 0.8, altitude 27,000 feet. The next section discusses the documentation of the can combustor performance at the four corners of the flight envelope.

4. CAN COMBUSTOR PERFORMANCE

After the design changes were complete, the can combustor performance at Mach 0.7 and 0.9, altitude 20,000 feet and 30,000 feet was defined. These tests were conducted with the baseline can design plus the shroud extension and the first stage air scoops described in Section IV.3.b. The fuel injection system used was the result of the combustion efficiency optimization tests of Section IV.2.

The combustion efficiency results are shown in Figure 30. Since the combustor could not be operated at the Mach 0.9, altitude 30,000 feet test condition, data was taken instead at a Mach 0.8, altitude

Figure 28. First Stage Pilot Can Air Scoops

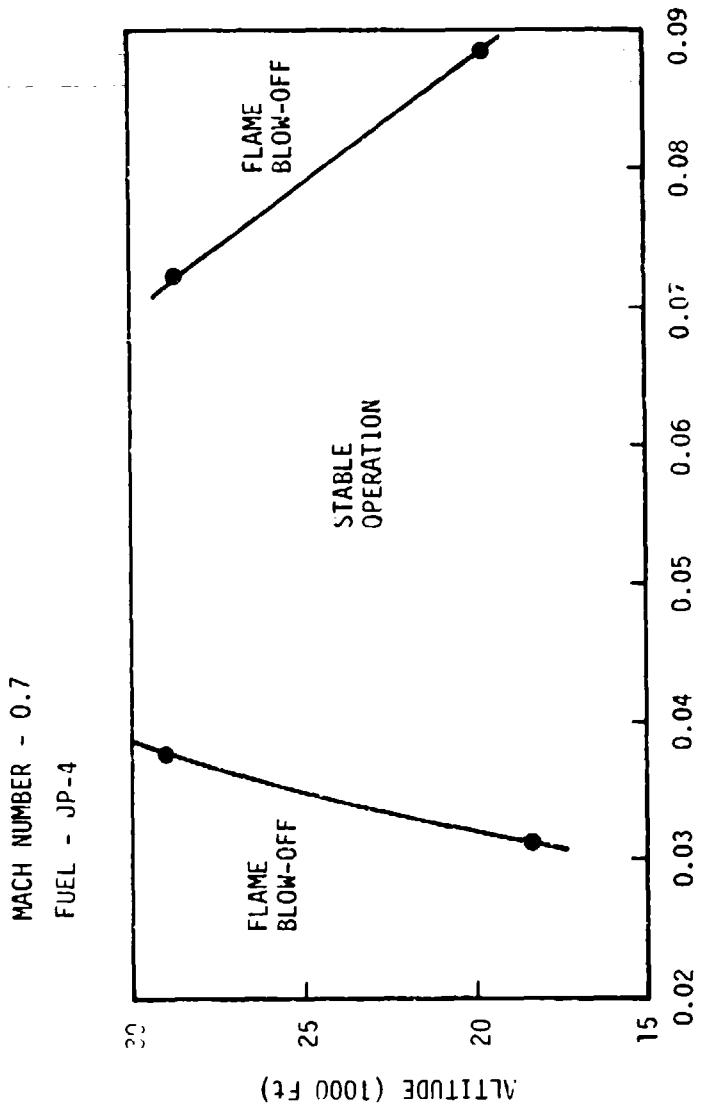

Figure 29. Stability Limits of Baseline Design with Shroud Extension and Air Scoops

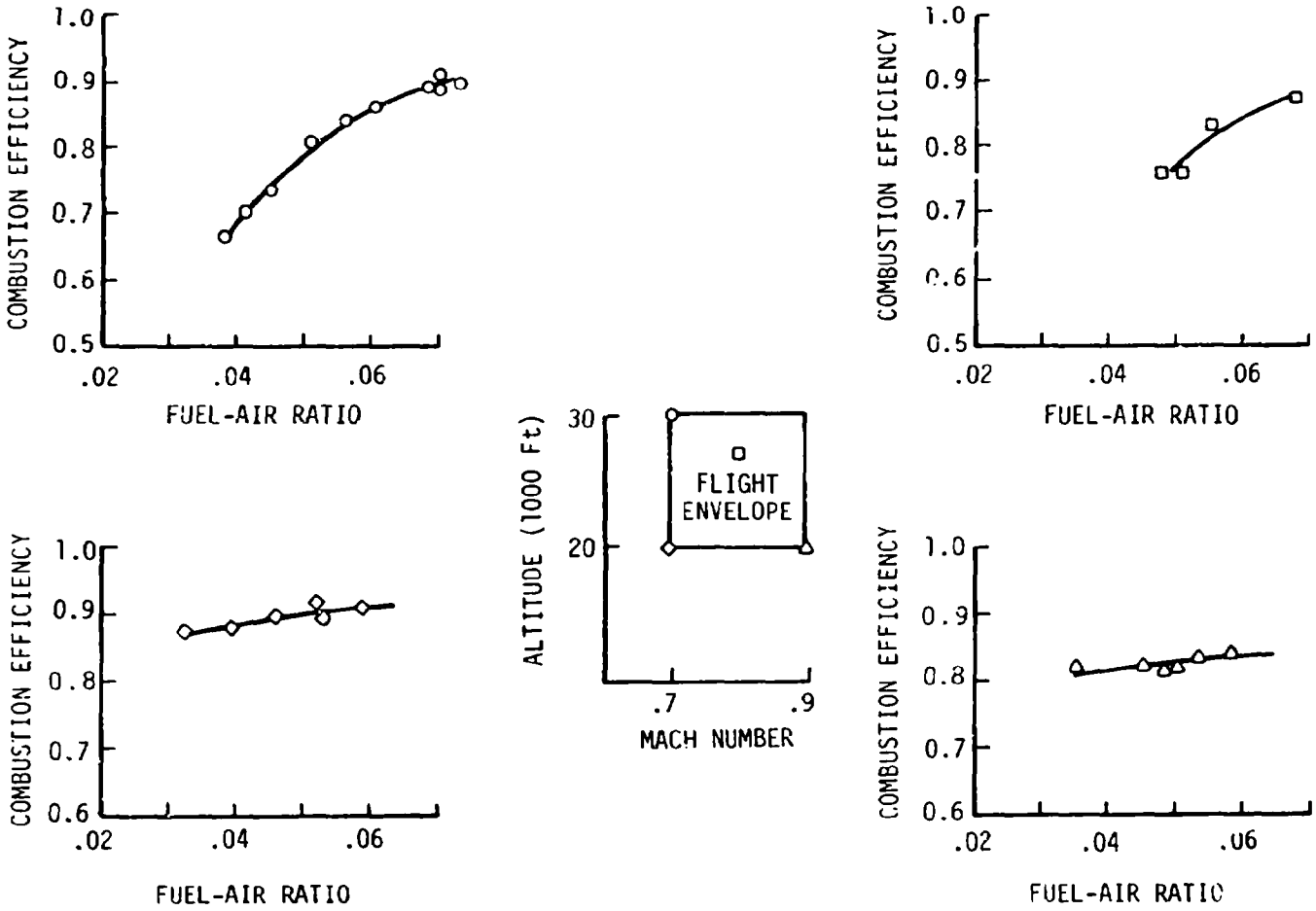

Figure 30. Combustion Efficiency vs. Engine Fuel-Air Ratio

27,000 feet test condition. In each of the four combustion efficiency curves, the lower fuel-air ratio is the lowest fuel-air ratio which would sustain combustion. The highest fuel-air ratio indicated on each curve is not the upper limit on sustained combustion. The combustor was not tested above a fuel-air ratio of 0.06 at the 20,000 feet test conditions due to the high engine tailpipe temperatures experienced at near stoichiometric combustion. In the test set-up, adequate tailpipe cooling was not available. However, there is no reason to believe, due to the near constant slope of the curves, that the combustion efficiency at the near stoichiometric fuel-air ratio would be much different in value. At the higher altitude test conditions, the fuel-air ratio was not extended much beyond the stoichiometric fuel-air ratio since the performance begins to drop off at this point. One can see that the higher combustor air flow velocities associated with low fuel-air ratios are much more critical at the higher altitude conditions. At the higher altitude conditions, combustion could not be sustained at the low fuel-air ratios.

Figure 31 shows the net jet thrust performance of the engine. The figure shows the increase in thrust due to higher dynamic pressures and higher mass flow rates associated with the higher Mach number test conditions. Also shown is the decrease in thrust with the lower pressures and lower mass flow rates associated with the higher altitude conditions.

The engine total pressure recovery is shown in Figure 32. The high pressure recoveries indicate that a low drag and low pressure loss design was achieved. Low pressure loss is very important in order that the thrust level can be as high as possible.

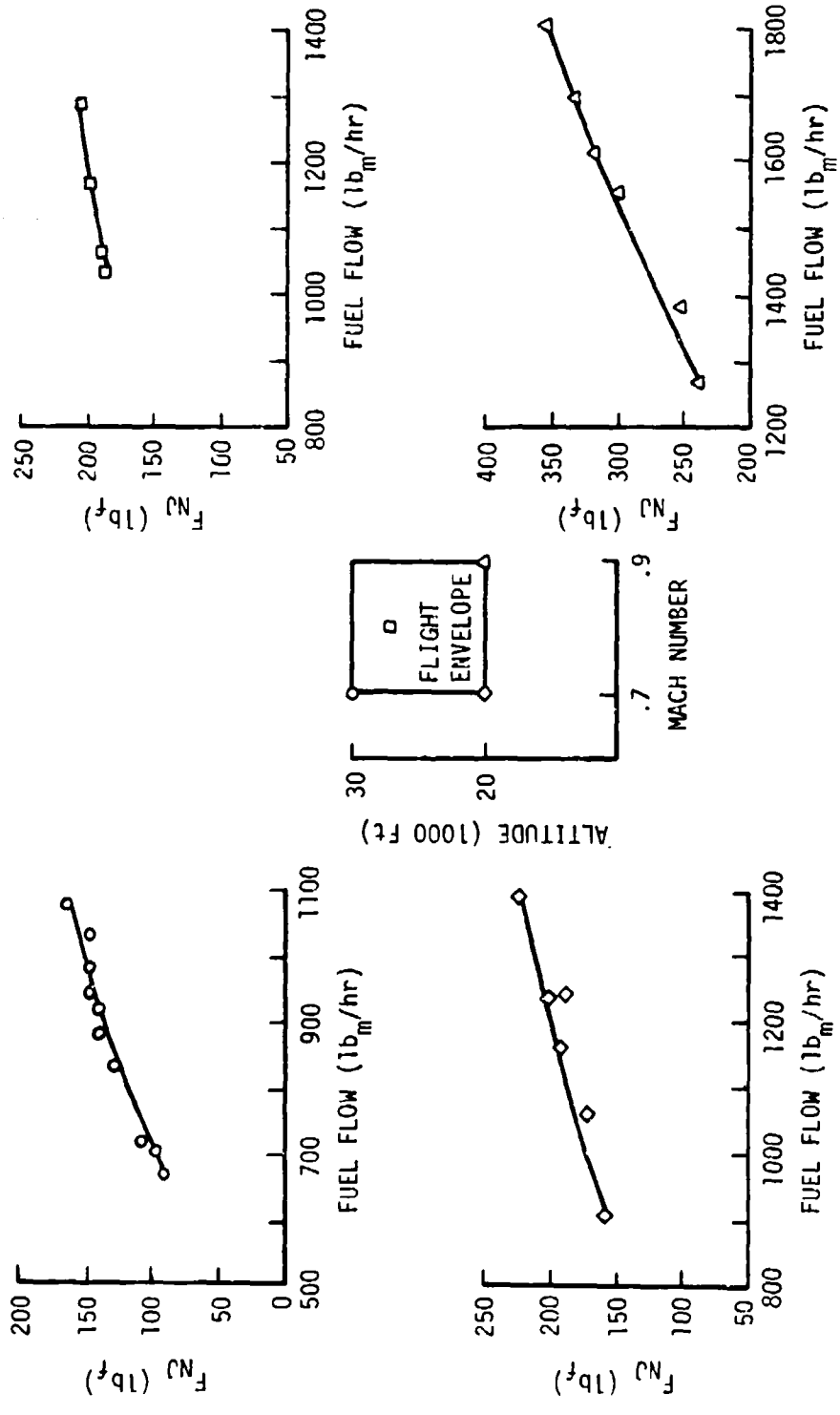

Figure 31. Net Jet Thrust vs. Engine Fuel Flow

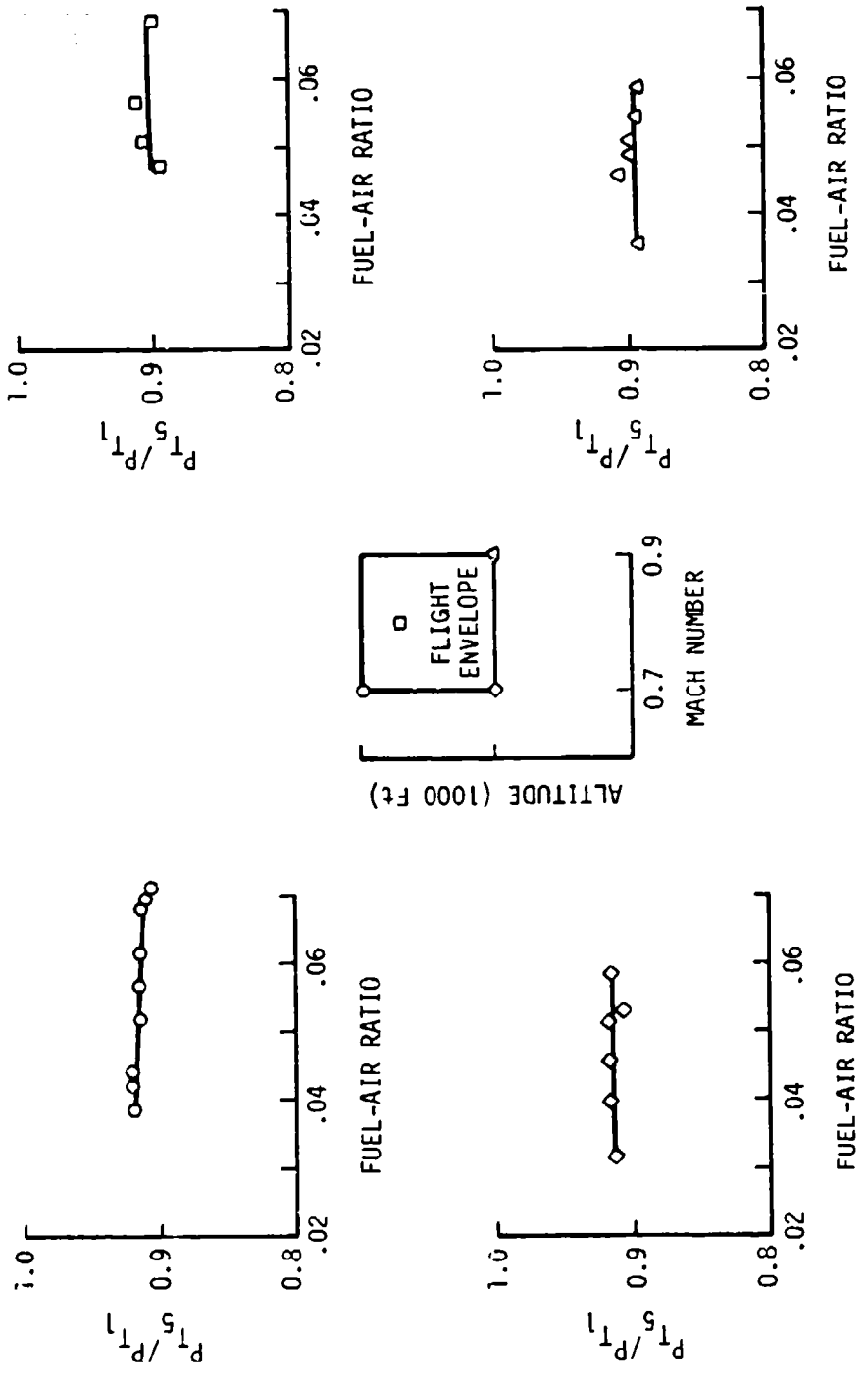

Figure 32. Total Pressure Recovery vs. Engine Fuel-Air Ratio

5. MODEL AND ACTUAL RAMJET THRUST PERFORMANCE COMPARISON

In order to show that the assumptions of the performance calculations were valid and the can combustor thrust performance was near the maximum performance which can be expected from the ramjet cycle for the combustion efficiencies obtained, the test data was plotted on model performance curves. The model predicted performance was obtained with use of the subsonic engine performance computer program of Reference 18. The engine burner drag coefficient was calculated from the test data to be 3.0. This burner drag coefficient and the actual engine dimensions were used to obtain a parametric plot of net jet thrust coefficient vs. specific fuel consumption for all fuel-air ratios and combustion efficiencies. This was done for each of the four test conditions, as shown in Figures 33, 34, 35, and 36. On each of the parametric plots the combustion efficiency obtained at a given fuel-air ratio in testing was plotted as a solid line. The solid lines thus represent the thrust performance of the model ramjet for the combustion efficiency ranges and fuel-air ratios that were obtained during testing. The actual thrust coefficient and specific fuel consumption test results are shown as data points on the figures. The only other factor which affects internal ramjet performance other than combustion efficiency is internal aerodynamics. The distance along the constant fuel-air ratio lines between the data points and the solid line represents the aerodynamic effects. At the Mach 0.7, altitude 20,000 and 30,000 feet test conditions and Mach 0.8, altitude 27,000 feet test condition (Figures 33, 34, and 35), the calculated thrust performance corresponds very well to the predicted values of the solid line. At the Mach 0.9, altitude 20,000 feet test condition (Figure 36), the calculated thrust and specific fuel consumption

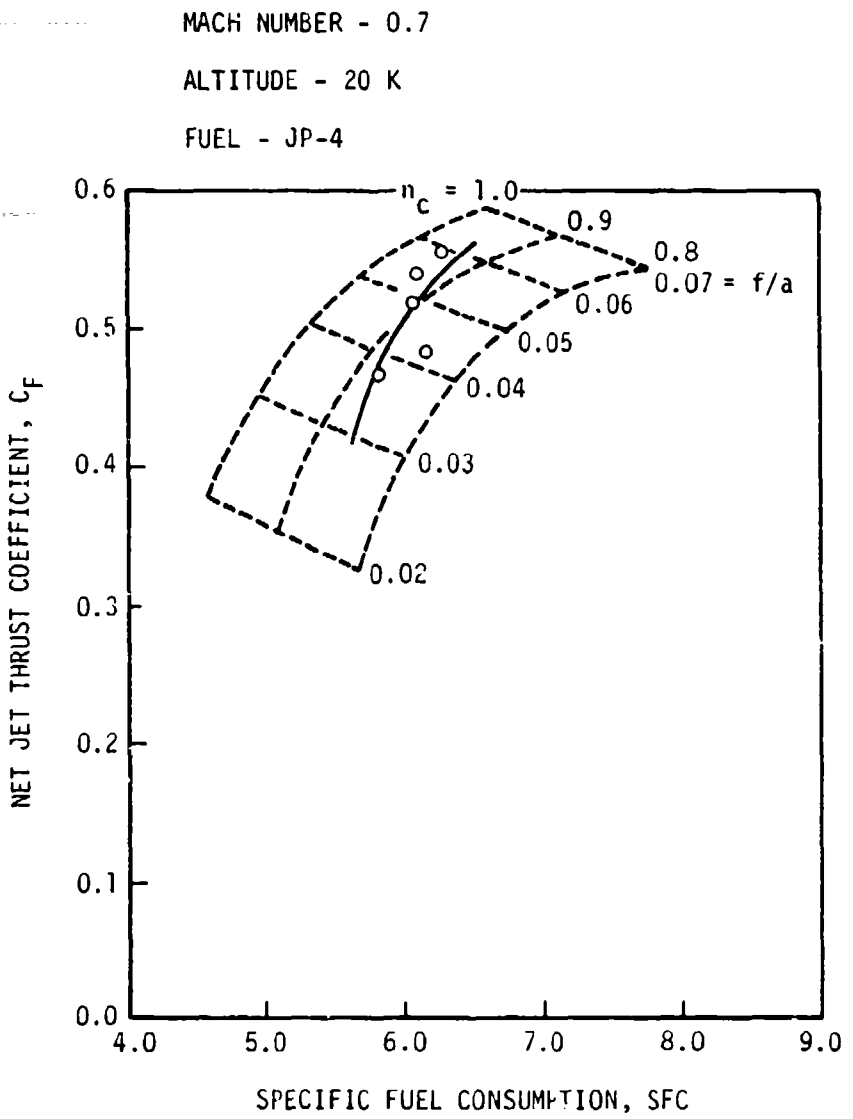

Figure 33. Model and Actual Thrust Performance

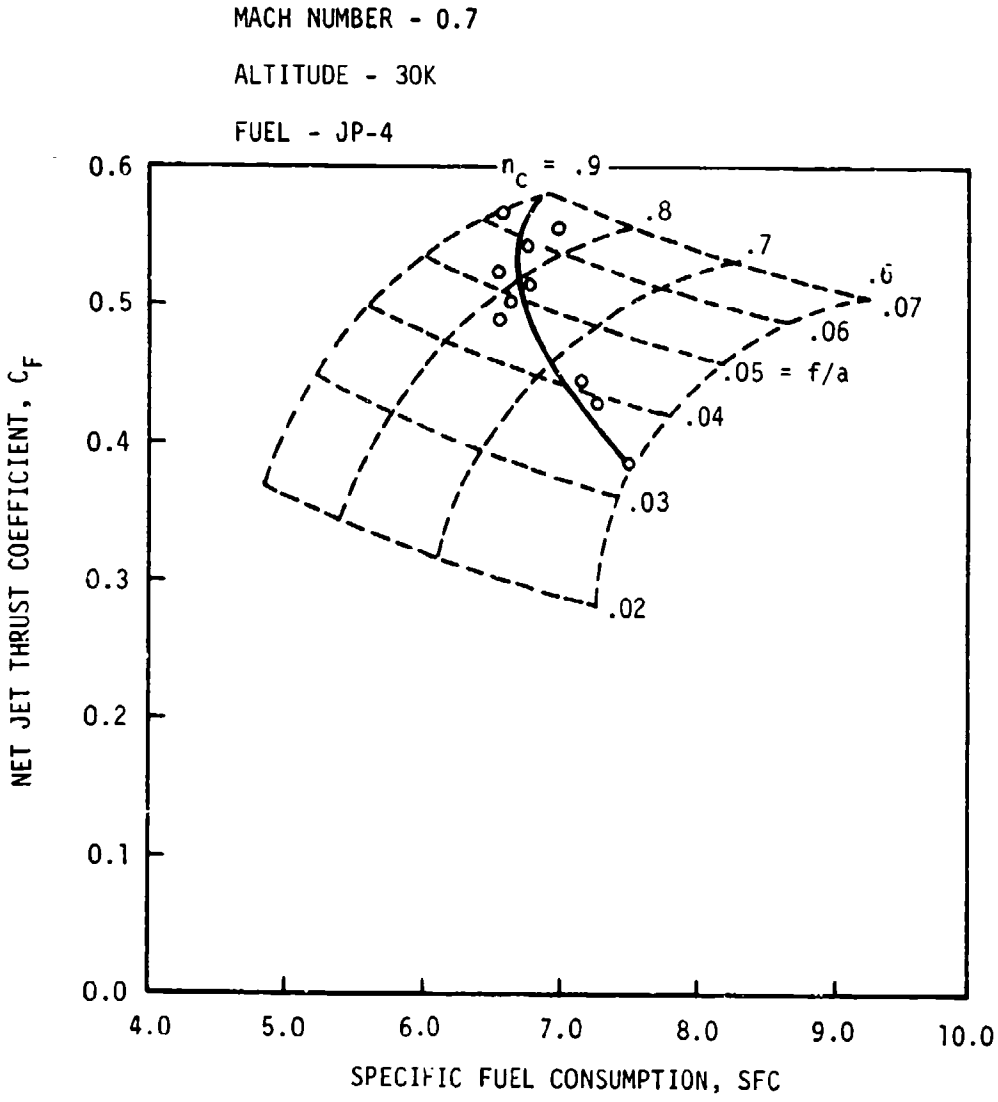

Figure 34. Model and Actual Thrust Performance

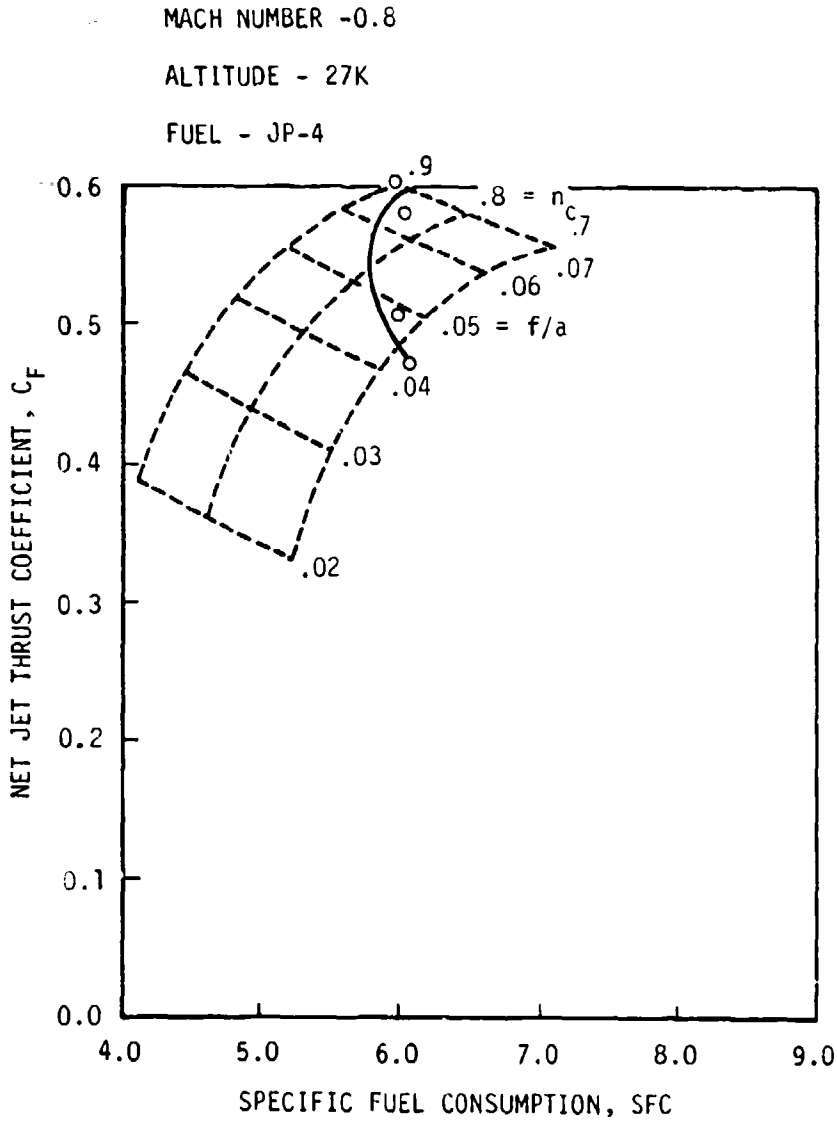

Figure 35. Model and Actual Thrust Performance

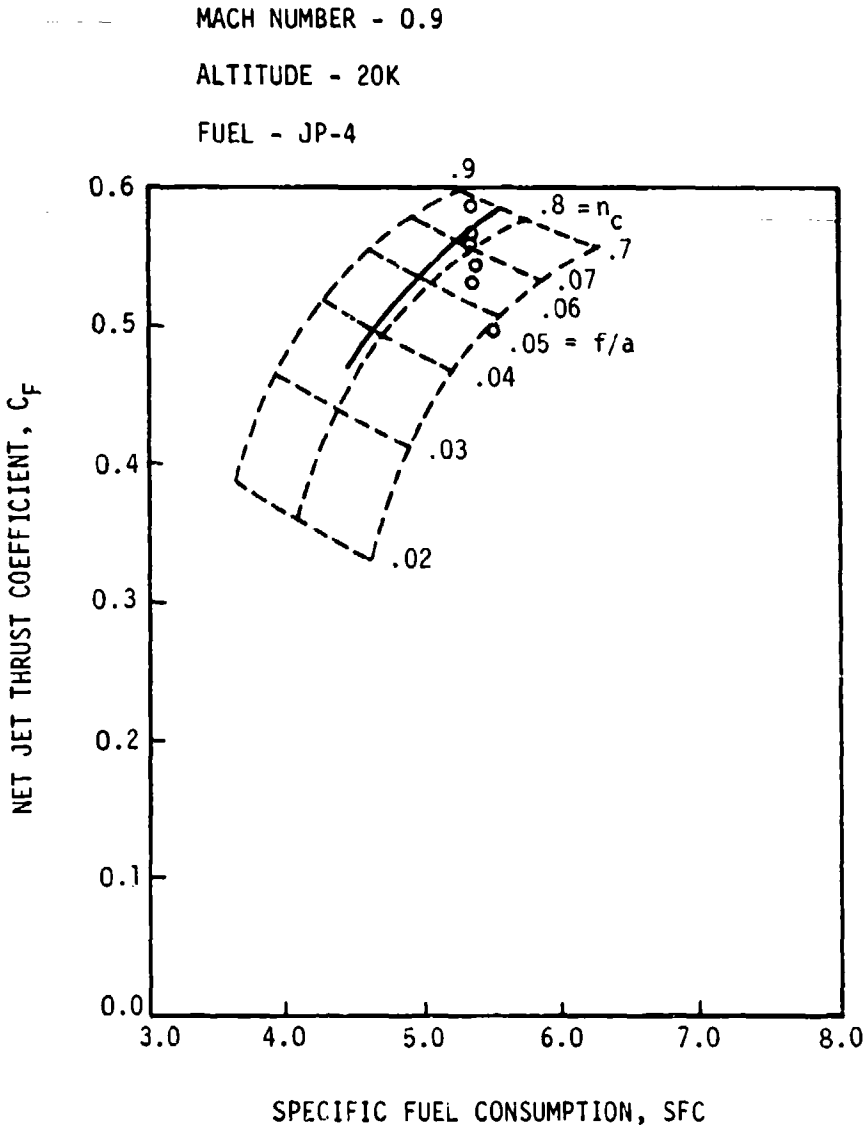

Figure 36. Model and Actual Thrust Performance

for the higher fuel-air ratios agreed with the predicted values. At the lower fuel-air ratios, aerodynamic losses lowered the thrust values even though good combustion efficiency was obtained.

SECTION V
CONCLUSIONS

The significant accomplishments of this study are summarized below:

1. A ramjet can combustor can be designed to operate in the flight envelope bounded by the flight conditions of Mach 0.7 and 0.9, altitude 20,000 feet, Mach 0.7, altitude 30,000 feet, and Mach 0.8, altitude 27,000 feet.

2. The design of the combustor can be free of close fabrication tolerance requirements, and combustion efficiencies of 80 to 90 percent are still attainable. Because of the uncomplicated design, the combustor can be easily and inexpensively placed in production.

3. In a can combustor designed to operate at pressures of one-half atmosphere and very low incoming air temperatures, the most important aspect is a well-designed piloting system.

4. Minimum burner drag, and thus low pressure drop, can be obtained by allowing a large total hole open area without sacrificing recirculation zone volume. This can be accomplished with two conical cans in series, which provides a large recirculation volume.

5. The fuel injection system is of great importance at the low temperature and pressure operating conditions. The fuel should be added near the center of the engine and allowed to spread radially to the outer stage air-entry holes of the combustor. The full-cone fuel nozzle provides better atomization and pilot combustor performance than the hollow-cone nozzle. The best overall combustion efficiency is obtained when the pilot can is operating at near stoichiometric.

6. The addition of air scoops on the first stage of air-entry holes increases the low pressure stable operation range of the can combustor.

7. The direct-connect pipe test set-up provides a valid performance evaluation of the subsonic ramjet engine. Dependable thrust calculations from pressure measurements can be made.

The final result of this program has been the direct-connect pipe testing of a subsonic ramjet engine with a can combustor. The program has demonstrated that the ramjet with a can combustor will provide an inexpensive propulsion system with modest performance characteristics.

REFERENCES

1. Watson, K. A., "X, Y, Z Mach Number Functions for One-Dimensional Compressible Flow", APRA-TM-70-16, May 1970.

2. Farley, J. M., Smith, R. E., and Dovolny, J. H., "Preliminary Experiments with Pilot Burners for Ramjet Combustors", NACA RM-E52J23, Lewis Research Center, Cleveland, Ohio, January, 1953.

3. Feleznik, F. J. and Gordon, S., "A General IBM 704 or 7090 Computer Program for Computation of Chemical Equilibrium Compositions, Rocket Performance, and Chapman-Jouguet Detonations", NASA TND-1454, Lewis Research Center, Cleveland, Ohio, October, 1962.

4. Gordon, S. and Feleznik, F. J., "A General Computation Program for Computation of Chemical Equilibrium Compositions, Rocket Performance, and Chapman-Jouguet Detonations; Supplement 1", NASA TND-1737, Lewis Research Center, Cleveland, Ohio, October 1963.

5. Ross, J. L., "A Fuel Data Standardization Study for JP-4, JP-5, JP-7, and RJ-5 Combusted in Air", AFAPL-TR-74-22, Wright-Patterson Air Force Base, Ohio, March, 1974.

6. DeZubay, E. A., "Characteristics of Disk Controlled Flame", Aero Digest, July 7, 1950, p. 54.

7. Longwell, J. P. and Weiss, M. A., "High Temperature Reaction Rates in Hydrocarbon Combustion", Ind. Eng. Chem., Vol. 47, August 4, 1955, p. 1634.

8. Zelinski, J. J., Mathews, L. J. III, Falk, F., and Bagnall, E. C., "The Design of Combustors for Ramjet Engines,", Combustion and Flame, Vol. 4, 1960, p. 343.

9. Ozawa, R. I., "Survey of Basic Data on Flame Stabilization and Propagation for High Speed Combustion Systems", AFAPL-TR-70-81, Wright-Patterson Air Force Base, Ohio, 1971.

10. Levenspiel, O., Chemical Reaction Engineering, John Wiley & Sons, Inc., 1962.

11. Vincenti, W. G., and Kruger, C. H., Physical Gas Dynamics, John Wiley & Sons, Inc., 1967, p. 210.

12. Edelman, R. and Fortune, O., "A Quasi-Global Chemical Kinetic Model for the Finite Rate Combustion of Hydrocarbon Fuels", AIAA 69-86.

13. Grobman, J. S., "Comparison of Calculated and Experimental Total Pressure Loss and Airflow Distribution in Tubular Turbojet Combustors with Tapered Liners", NASA TM-11-26-58E, 1959.

REFERENCES (Concluded)

14. Dittrich, R. T. and Graves, C. C., "Discharge Coefficients for Combustor-Liner Air-Entry Holes", NACA Technical Note 3663, April, 1956.

15. Shapiro, A. H., The Dynamics and Thermodynamics of Compressible Fluid Flow, Vol. I, The Ronald Press Company, 1953.

16. Zucrow, M. J., Aircraft and Missile Propulsion, Vol. II, John Wiley and Sons, Inc., 1964.

17. Benedict, R. P., Fundamentals of Temperature, Pressure, and Flow Measurements, John Wiley and Sons, Inc., 1969.

18. Hornbeck, C. E., Can-Type Combustor Design and Evaluation for a Low Cost Ramjet, Thesis: The Ohio State University, 1975.

☆ U. S. GOVERNMENT PRINTING OFFICE: 1976 — 657-650/480